The Geometry of Reaction Dynamics

T. Uzer
Center for Nonlinear Sciences, School of Physics
Georgia Institute of Technology
Atlanta, GA 30332-0430, USA

Charles Jaffé
Department of Chemistry
West Virginia University
Morgantown, WV 26506-6045, USA

Jesús Palacián, Patricia Yanguas
Departamento de Matemática e Informática
Universidad Pública de Navarra
31006 - Pamplona, Spain

Stephen Wiggins
School of Mathematics
University of Bristol
Bristol, BS8 1TW, UK

July 25, 2001

Abstract

The geometrical structures which regulate transformations in dynamical systems with three or more degrees of freedom form the subject of this paper. Our treatment focusses on the $2n-3$ dimensional normally hyperbolic invariant manifold (NHIM) in n-degree-of-freedom systems associated with a center $\times \cdots \times$ center $\times$ saddle in the phase space flow in the $2n-1$ dimensional energy surface. The NHIM bounds a $2n-2$ dimensional surface, called a "transition state" in chemical reaction dynamics, which partitions the energy surface into volumes characterized as "before" and "after" the transformation. This surface is the long-sought momentum-dependent transition state beyond two degrees of freedom. The $2n-2$ dimensional stable and unstable manifolds associated with the $2n-3$ dimensional NHIM are impenetrable barriers with the topology of multidimensional spherical cylinders. The phase flow interior to these spherical cylinders passes through the transition state as the system undergoes its transformation. The phase flow exterior to these spherical cylinders is directed away from the transition state and, consequently, will never undergo the transition. The explicit forms of these phase space barriers can be evaluated using normal form theory. Our treatment has the advantage of supplying a practical algorithm, and we demonstrate its use on a strongly coupled nonlinear Hamiltonian, the hydrogen atom in crossed electric and magnetic fields.

1 Introduction

In this article we develop a general formulation of the nonlinear dynamics and geometry of classical reaction dynamics. Our formalism hinges on finding, for the first time, the dynamically exact higher dimensional structures (separatrices, dividing surfaces) which regulate transport between qualitatively different states ("reactants" and "products") in three or more degrees of freedom. The work explained in this article has been a longstanding and often-expressed aspiration of the science and mathematics communities, but it is only now that we have the theoretical and computational tools for its fulfillment.

The central concept in this formulation is the so-called transition state, which has its origin in the theory of chemical reaction dynamics [30], see also [46]. This theory stipulates a minimal set of states that all reactive trajectories must pass through and which is never encountered by any nonreactive trajectories. This set of states is collectively called the "transition state." Transition State Theory (TST) was developed in the 1930s [30] as a way to determine absolute chemical reaction rates. The dominant formulation of the theory for many decades was an essentially thermodynamic picture due to Eyring [13]. However, Wigner [64] developed a rival, dynamical picture in parallel with Eyring's work. Wigner's formulation shows clearly that the transition state (TS) is a general property of all dynamical systems, provided that they evolve from "reactants" to "products" [63]. The TS, therefore, is not confined to chemical reaction dynamics [41], but it also controls transition rates in many interesting systems, including, e.g., the rearrangements of clusters [24], the ionization of atoms [27], conductance due to ballistic electron transport through microjunctions [12], and diffusion jumps in solids [53].

Historically, the notion of a transition state makes its first appearance in the work of Marcelin [37] in 1915. After a hiatus, in 1931, Eyring and Polanyi [14] quantified the idea of a transition state in the collinear H + H_2 reaction. Their paper, which most regard as the origin of modern chemical reaction theory, reports the first calculation of the potential energy surface of a reaction. This two-dimensional surface consists of two valleys, associated with the reactants and the products, respectively, and which are separated by a col or saddle. Using this surface, Eyring and Polanyi define the transition state as the path of steepest ascent from the saddle point of the barrier. After the system has crossed the transition state, the forces are such that they push the system even farther out into the products valley. Thus, it would appear that the system can never recross the transition state to return to the reactants side of the potential, in other words, that the transition state is a surface of no return.

However, even in the earliest days it was recognized that the transition state as defined by Eyring and Polanyi was in fact not a surface of no return [25]. This is due to dynamical effects that result from cross-terms in the kinetic energy, for example, dynamical barriers [6]. Enforcing this "no recrossing" requirement has been a major obstacle to applying TST in strongly coupled, multidimensional systems.

The recognition of the intricate nature of the dynamics led to the development of a variational approach [26], [33], [29]. Here one considers the set of all possible transition states and then chooses the one with the minimum flux across it. Clearly, if trajectories recross a transition state candidate, these trajectories will be counted more than once in the computation of the flux, leading to an overestimation of the classical rate. Pechukas [44] solved the variational problem for systems with two degrees of freedom by proving that the surface of minimum flux, and hence the transition state, must be an unstable periodic orbit whose projection into coordinate space connects the two branches of the relevant equipotentials. These surfaces are called "periodic orbit dividing surfaces" or PODS (both singular and plural). The PODS with the minimum flux is chosen as the transition state.

While the original idea of a transition state was expressed as a dividing surface in *configuration*

space it was soon recognized that a proper treatment must be in terms of dividing surfaces in *phase space*. But how does one partition multidimensional phase space cleanly into volumes containing reactants and products alone? Progress in this direction had to wait for two developments, (i) advances in the study of multidimensional dynamical systems, and (ii) computing power. In the mid 1980's Davis and co-workers [7] studied the phase space dynamics of a number of reactive systems. They showed that the partitioning of phase space can be accomplished using the manifolds of the PODS associated with the transition states. Jaffé and co-workers [52] have extended these ideas considerably and have shown that the manifolds of the PODS can be used to construct an invariant fractal tiling of phase space and in the simplest case of complex formation (unimolecular reactions) have characterized this fractal structure.

Pechukas' prescription for the construction of the PODS involves potential energy surfaces. Jaffé et al. [27] have shown that in systems with velocity dependent forces (e.g., Coriolis forces), where defining a potential energy is problematical, one can still construct PODS by the judicious choice of coordinates. However, even after these advances, a serious obstacle remained to the further development of transition state theory, namely the lack of understanding of the geometry of higher dimensional phase space. Consequently, TST has remained confined to low dimensions for which the dividing surfaces can be found in practice. We overcome this obstacle in the present article.

In what follows, we will present a general formulation of the phase space geometry that underlies the classical theory of multidimensional chemical reaction theory. Our article is organized as follows. In Section 2 we develop the rigorous mathematical theory of the geometry of higher dimensional saddles and their associated separatrices in the context of the theory of normally hyperbolic invariant manifolds. In Section 2.1 we develop the theory for a class of linear Hamiltonian systems. The linear systems contain the essence of the geometrical features contained in nonlinear systems and also provide the important advantage of being able to represent all the relevant surfaces (e.g., the normally hyperbolic invariant manifold (NHIM), its stable and unstable manifolds, and the transition state) as explicit formulae. This is a tremendous intuitive aid in getting the correct "dimension count" as well as precisely describing the nature of trajectories near these surfaces in terms of coordinates. The intuition and analytical approach obtained in this way is invaluable for understanding the nonlinear problem as it is very easy to fool oneself with general geometrical arguments in higher dimensional systems. In Section 2.2 we develop the theory for nonlinear Hamiltonian systems. First, we show that near an equilbrium point of saddle $\times$ center $\times \cdots \times$ center stability type the Hamiltonian can be transformed to a normal form where the normally hyperbolic invariant manifold, its stable and unstable manifolds, and the transition state are trivial to obtain analytically. Moreover, if there are nonresonance conditions satisfied for the center type coordinates, the normal form, truncated at any finite order, is integrable. The theory we develop provides an algorithmic procedure for identifying the transition state and describing the local geometry of trajectories. In Section 3 we illustrate the theory by applying it to the hydrogen atom in crossed electric and magnetic fields [48], [49], [54]. We choose this system because it encapsulates all key ingredients of transition state theory as well as raising a number of issues that are not normally encountered when applying conventional configuration space transition state theory to chemical reactions: velocity dependent forces, which can be traced directly to the presence of the magnetic field, preclude the definition of a potential, and require that the transition state be in phase rather than configuration space [27].

2 Phase Space Structure and the Transition State for a Class of n-Degree-of-Freedom Hamiltonians

In this section we will develop the phase space structure for a broad class of n-degree-of-freedom Hamiltonian systems that are appropriate for the study of reaction dynamics. For this class of systems we will show that on the energy surface there is always a higher dimensional version of a "saddle" (a normally hyperbolic invariant manifold (NHIM) [61]) with codimension one stable and unstable manifolds. Within a region bounded by the stable and unstable manifolds of the NHIM we can construct the transition state which is a dynamical surface of no return for the trajectories. Our approach is algorithmic in nature in the sense that we provide a series of steps that can be carried out to locate the NHIM, its stable and unstable manifolds, the transition state, as well as describe all possible trajectories near the transition state.

We will begin by giving a detailed study of a class of n-degree-of-freedom *linear* Hamiltonian systems because it contains the essential geometrical features of the nonlinear system and also carries with it the intuitive advantage of enabling us to represent all of the geometrical objects with explicit formulae.

2.1 Phase Space Structure and the Transition State for a Class of n-Degree-of-Freedom Linear Hamiltonian Systems

Consider a quadratic Hamiltonian of the following form:

$$H = \frac{1}{2}\sum_{i=1}^{n} p_i^2 + \frac{1}{2}\sum_{i=1}^{n-1} \omega_i^2 q_i^2 - \frac{\lambda^2}{2} q_n^2, \qquad (q_1, \ldots, q_n, p_1, \ldots, p_n) \in \mathbb{R}^{2n}, \tag{1}$$

with the corresponding Hamiltonian vector field given by:

$$\begin{aligned}
\dot{q}_i &= \frac{\partial H}{\partial p_i} = p_i, \\
\dot{p}_i &= -\frac{\partial H}{\partial q_i} = -\omega_i^2 q_i, \qquad i = 1, \ldots, n-1, \\
\dot{q}_n &= \frac{\partial H}{\partial p_n} = p_n, \\
\dot{p}_n &= -\frac{\partial H}{\partial q_n} = \lambda^2 q_n.
\end{aligned} \tag{2}$$

This system consists of $n-1$ uncoupled linear oscillators, with the remaining uncoupled degree-of-freedom consisting of a parabolic barrier. In the language of reaction dynamics, the coordinates (q_n, p_n) are the reaction coordinates and the remaining coordinates are referred to as the bath coordinates.

On the $2n-1$ dimensional energy surface defined by:

$$\frac{1}{2}\sum_{i=1}^{n} p_i^2 + \frac{1}{2}\sum_{i=1}^{n-1} \omega_i^2 q_i^2 - \frac{\lambda^2}{2} q_n^2 = h = constant, \tag{3}$$

we can speak of the energy in each DOF separately. Accordingly, we have the following notation:

$$\frac{1}{2}\left(p_k^2 + \omega_k^2 q_k^2\right) = E_k, \quad k = 1, \ldots n-1, \qquad \frac{1}{2}\left(p_n^2 - \lambda^2 q_n^2\right) = E_n, \tag{4}$$

where

$$h = E_1 + \cdots + E_n. \tag{5}$$

In Fig. 1 we illustrate the phase space structure of the n uncoupled systems.

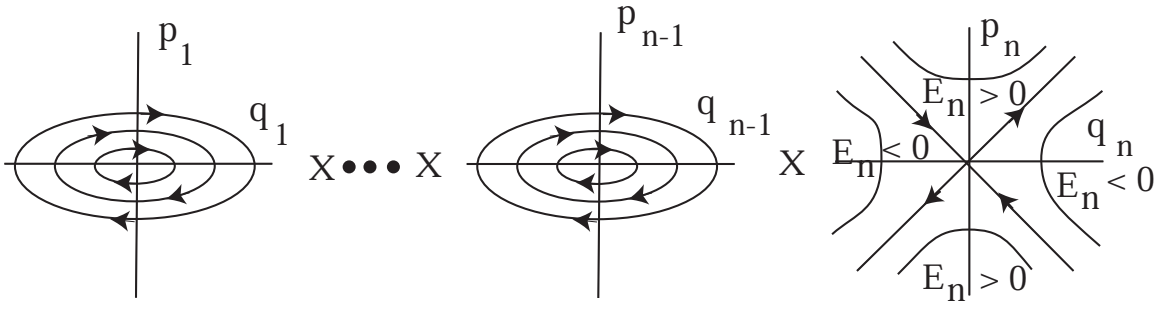

Figure 1: Phase portrait for the uncoupled saddle and oscillators. In the phase portrait for the saddle the regions of positive and negative energy are denoted. The separatrices have zero energy.

In the $q_n - p_n$ phase portrait the trajectories that go from positive to negative q_n (or vice versa) are said to undergo reaction. These are the trajectories with $E_n > 0$ in Fig. 1. This figure shows that there are two types of *reactive trajectories*. Those with $p_n > 0$, which are referred to as the *forward reactive trajectories* and those with $p_n < 0$ which are referred to as the *backward reactive trajectories*. Notice that the p_n component of a reactive trajectory cannot change sign during its evolution. The trajectories with $E_n < 0$ are referred to as *nonreactive trajectories*.

2.1.1 The Energy Surface

The dynamics occurs within the $2n-1$ dimensional energy surface. If we rewrite (3) as:

$$\frac{1}{2}\sum_{i=1}^{n} p_i^2 + \frac{1}{2}\sum_{i=1}^{n-1} \omega_i^2 q_i^2 = h + \frac{\lambda^2}{2} q_n^2, \tag{6}$$

the geometry of the energy surface becomes a bit clearer. Namely, we can view it as a "$(2n-2)$ sphere" in $q_1 - p_1 \cdots q_n - p_n$ space with "radius" $h + \frac{\lambda^2}{2} q_n^2$. In this case the radius of the $(2n-2)$ sphere will vary as the trajectory evolves in time. Hence, we can view the energy surface as $S^{2n-2} \times \mathbb{R}$. The explicit map from the energy surface in $\mathbb{R}^{2n}$ into $S^{2n-2} \times \mathbb{R}$ is essentially obvious from the formula. For each $q_n \in \mathbb{R}$, we have a map of $(q_1, p_1, \ldots, q_{n-1}, p_{n-1}, p_n)$ into S^{2n-2} defined by:

$$(q_1, p_1, \ldots, q_{n-1}, p_{n-1}, p_n) \mapsto \frac{1}{2}\sum_{i=1}^{n} p_i^2 + \frac{1}{2}\sum_{i=1}^{n-1} \omega_i^2 q_i^2 = h + \frac{\lambda^2}{2} q_n^2.$$

2.1.2 The Normally Hyperbolic Invariant Manifold (NHIM) and its Stable and Unstable Manifolds

Note that if we set $q_n = p_n = 0$ in (2) then $\dot{q}_n = \dot{p}_n = 0$. Therefore $q_n = p_n = 0$ is a $2n-2$ dimensional invariant manifold. The intersection of this invariant manifold with the energy surface is obtained by setting $q_n = p_n = 0$ in (3), which gives:

$$\frac{1}{2}\sum_{i=1}^{n-1} p_i^2 + \frac{1}{2}\sum_{i=1}^{n-1} \omega_i^2 q_i^2 = h = constant. \tag{7}$$

For $h > 0$ this is the equation of a $2n-3$ dimensional sphere, denoted S_h^{2n-3}. It is an example of a *normally hyperbolic invariant manifold* (NHIM) [61]. This means that the stretching and contraction rates under the linearized dynamics transverse to the sphere dominate those tangent to the sphere. This is clear for this example since the dynamics normal to the sphere are described by the exponential contraction and expansion of the saddle-point dynamics in the $q_n - p_n$ variables. Hence the sphere acts as a "big saddle point". (See [61] for a detailed discussion of normally hyperbolic invariant manifolds.) This sphere has $(2n-2)$-dimensional stable and unstable manifolds, denoted $W^s\left(S_h^{2n-3}\right)$ and $W^u\left(S_h^{2n-3}\right)$, respectively, which act as separatrices in the $(2n-1)$-dimensional energy surface, since they are of one less dimension. These manifolds are given by:

$$\begin{aligned} W^s\left(S_h^{2n-3}\right) &= \left\{(q_1,\ldots,q_n,p_1,\ldots,p_n)\,|\,\frac{1}{2}\sum_{i=1}^{n-1} p_i^2 + \frac{1}{2}\sum_{i=1}^{n-1} \omega_i^2 q_i^2 = h,\, p_n = -\lambda q_n\right\}, \\ W^u\left(S_h^{2n-3}\right) &= \left\{(q_1,\ldots,q_n,p_1,\ldots,p_n)\,|\,\frac{1}{2}\sum_{i=1}^{n-1} p_i^2 + \frac{1}{2}\sum_{i=1}^{n-1} \omega_i^2 q_i^2 = h,\, p_n = \lambda q_n\right\}. \end{aligned} \tag{8}$$

From these equations it is clear that the stable and unstable manifolds of the sphere have the structure of $S^{2n-3} \times \mathbb{R}$, which we refer to as *spherical cylinders*. Note that the stable and unstable manifolds of S_h^{2n-3} have the same energy as S_h^{2n-3} since the lines $p_n = -\lambda q_n$ and $p_n = \lambda q_n$ have zero energy. They act as boundaries between the reactive and nonreactive trajectories.

In the language of dynamical systems theory both the stable and unstable cylinders have two "branches" corresponding to $p_n > 0$ and $p_n < 0$. In the language of reaction dynamics these two branches are related to the forward and backward reactions. Consequently, it is useful to develop notation for the two branches of the stable and unstable cylinders. Accordingly, we make the following definitions.

The forward stable cylinder:

$$W_f^s(S_h^{2n-3}) = \left\{(q_1,p_1,\ldots,p_n,q_n)|\frac{1}{2}\sum_{i=1}^{n-1} p_i^2 + \frac{1}{2}\sum_{i=1}^{n-1} \omega_i^2 q_i^2 = h,\, p_n = -\lambda q_n > 0\right\}. \tag{9}$$

The backward stable cylinder:

$$W_b^s(S_h^{2n-3}) = \left\{(q_1,p_1,\ldots,p_n,q_n)|\frac{1}{2}\sum_{i=1}^{n-1} p_i^2 + \frac{1}{2}\sum_{i=1}^{n-1} \omega_i^2 q_i^2 = h,\, p_n = -\lambda q_n < 0\right\}. \tag{10}$$

The forward unstable cylinder:

$$W_f^u(S_h^{2n-3}) = \left\{(q_1,p_1,\ldots,p_n,q_n)|\frac{1}{2}\sum_{i=1}^{n-1} p_i^2 + \frac{1}{2}\sum_{i=1}^{n-1} \omega_i^2 q_i^2 = h,\, p_n = \lambda q_n > 0\right\}. \tag{11}$$

The backward unstable cylinder:

$$W_b^u(S_h^{2n-3}) = \left\{(q_1,p_1,\ldots,p_n,q_n)|\frac{1}{2}\sum_{i=1}^{n-1} p_i^2 + \frac{1}{2}\sum_{i=1}^{n-1} \omega_i^2 q_i^2 = h,\, p_n = \lambda q_n < 0\right\}. \tag{12}$$

2.1.3 The Relation of the Normally Hyperbolic Invariant Spheres to the Center Manifold of the Origin

The Hamiltonian vector field (2) has an equilibrium point at the origin which has a $2n-2$ dimensional center manifold given by $p_n = q_n = 0$, a one dimensional stable manifold given by $q_i = p_i = 0$, $i = 1, \ldots, n-1$, $p_n = -\lambda q_n$, and a one dimensional unstable manifold given by $q_i = p_i = 0$, $i = 1, \ldots, n-1$, $p_n = \lambda q_n$. It is easy to check that the stable and unstable manifolds of the origin have the same energy as the origin, i.e., $h = 0$. We say that they are *isoenergetic*. However, the center manifold of the origin is not isoenergetic. The intersection of the center manifold of the origin with the energy surface is given by:

$$\frac{1}{2}\sum_{i=1}^{n-1} p_i^2 + \frac{1}{2}\sum_{i=1}^{n-1} \omega_i^2 q_i^2 = h = constant.$$

This is the normally hyperbolic invariant $2n-3$ dimensional sphere we described earlier. Hence we see that the center manifold of the origin is foliated by a one-parameter (normally the energy) family of normally hyperbolic invariant $2n-3$ dimensional spheres.

2.1.4 The Transition State

Now we construct the *transition state*. The transition state will have the following properties.

- It will be of dimension $2n-2$ in the $2n-1$ dimensional energy surface.
- Trajectories that cross the transition state correspond to reactive trajectories.
- The $2n-3$ dimensional saddle sphere will play an important role in the construction of the transition state.
- The transition state is a true "surface of no return" for this linear Hamiltonian system.

The transition state for this system is obtained by setting $q_n = 0$. If one looks at the line $q_n = 0$ in the $q_n - p_n$ phase plane in Fig. 1 on sees that this corresponds to initial conditions for all the trajectories that undergo reaction, with the exception of the saddle-point at the origin.

Now we look at this in the full $2n$-dimensional phase space. Setting $q_n = 0$ on the energy surface gives the equation:

$$\frac{1}{2}\sum_{i=1}^{n} p_i^2 + \frac{1}{2}\sum_{i=1}^{n-1} \omega_i^2 q_i^2 = h = constant. \tag{13}$$

This is the transition state. It is a $2n-2$ dimensional sphere. The sphere has two "halves"; $p_n > 0$ and $p_n < 0$. The sphere is divided into these two halves by $p_n = 0$, which corresponds to the saddle sphere S_h^{2n-3}. All reacting trajectories must pass through this transition state. The forward reactive trajectories pass through the sphere with $p_n > 0$ and the backward reactive trajectories pass through the sphere with $p_n < 0$.

This sphere is the higher dimensional analog of the "periodic orbit dividing surfaces"(PODS), see [45], which are built on unstable periodic orbits riding the ridges through saddle points in two degree-of-freedom systems ('2dof'). That the sphere (13) is a true surface of no return is proved as follows.

Theorem 2.1 *The $2n-2$ dimensional sphere given in (13) is a surface of no return for the trajectories of Hamilton's equations given in (2),* except *for trajectories starting on the invariant $2n-3$ dimensional sphere given in (7).*

Proof: The $2n-2$ dimensional sphere in the energy surface is defined by $q_n = 0$. If we examine Hamilton's equations (2) we see that $\dot{q}_n = p_n$. Hence q_n is always increasing (resp. decreasing) for $p_n > 0$ (resp. $p_n < 0$). Therefore trajectories starting on (13) with $p_n \neq 0$ (i.e., they are not on the $2n-3$ dimensional invariant sphere (7)) always leave (13) and can never return. □

2.1.5 The Reactive Trajectories and the Geometrical Role of the Stable and Unstable Spherical Cylinders

Now we examine more closely the role of the stable and unstable cylinders in defining the region of trajectories that undergo reaction. Let's rewrite the equation for the energy surface as follows:

$$\frac{1}{2}\sum_{i=1}^{n-1}\left(p_i^2 + \omega_i^2 q_i^2\right) + \frac{1}{2}\left(p_n - \lambda q_n\right)\left(p_n + \lambda q_n\right) = h.$$

The trajectories that undergo reaction satisfy:

$$0 < \frac{1}{2}p_i^2 + \frac{1}{2}\omega_i^2 q_i^2 = E_i < h, \quad i = 1, \ldots n-1, \qquad \frac{1}{2}\left(p_n - \lambda q_n\right)\left(p_n + \lambda q_n\right) = E_n > 0, \tag{14}$$

with

$$\sum_{i=1}^{n} E_i = h.$$

Now in order to have $\left(p_n - \lambda q_n\right)\left(p_n + \lambda q_n\right) > 0$ we must have:

$$p_n - \lambda q_n > 0, \qquad p_n + \lambda q_n > 0, \quad (\Rightarrow\ p_n > 0, \quad \text{forward reactive region}), \tag{15}$$

or

$$p_n - \lambda q_n < 0, \qquad p_n + \lambda q_n < 0, \quad (\Rightarrow\ p_n < 0, \quad \text{backward reactive region}). \tag{16}$$

The boundary of the region defined by (15) is given by:

$$p_n = -\lambda q_n, \quad p_n = \lambda q_n, \quad p_n > 0,$$

which is $W_f^s(S_h^{2n-3})$ and $W_f^u(S_h^{2n-3})$. The boundary of the region defined by (16) is given by:

$$p_n = -\lambda q_n, \quad p_n = \lambda q_n, \quad p_n < 0,$$

which is $W_b^u(S_h^{2n-3})$ and $W_b^s(S_h^{2n-3})$. These different regions are described geometrically in Fig. 2.

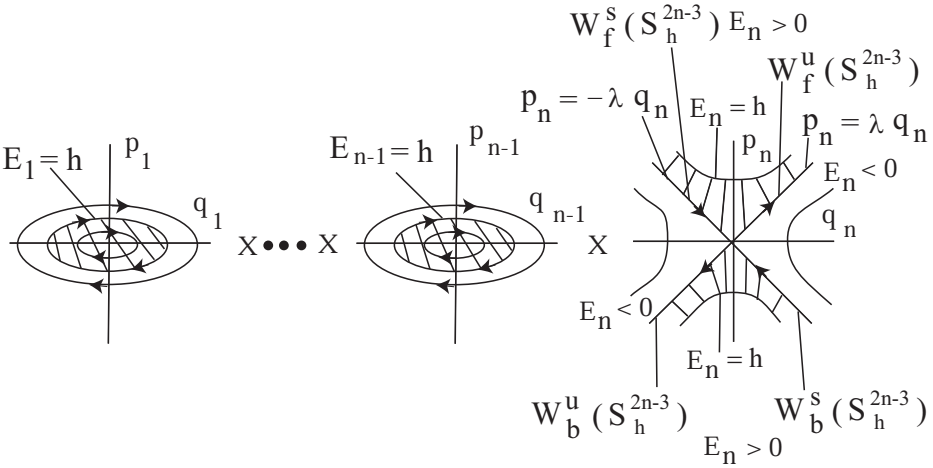

Figure 2: The reactive region with total energy h denoted by the cross-hatching. The forward reactive region ($p_n > 0$) is bounded by $W_f^s(S_h^{2n-3})$ and $W_f^u(S_h^{2n-3})$. The reverse reactive region ($p_n < 0$) is bounded by $W_b^u(S_h^{2n-3})$ and $W_b^s(S_h^{2n-3})$.

2.1.6 The Reactant and Product Segments of the Reactive Trajectories

Thus far, we have established the following.

- The forward reactive trajectories satisfy $E_n > 0$ and lie in the region bounded by $W_f^s(S_h^{2n-3})$ and $W_f^u(S_h^{2n-3})$ and the reverse reactive trajectories satisfy $E_n > 0$ and lie in the region bounded by $W_b^u(S_h^{2n-3})$ and $W_b^s(S_h^{2n-3})$.
- All reactive trajectories pass through the transition state, $q_n = 0$.

Now we want to describe the geometry of the reactive trajectories in more detail. In particular, for a given reactive trajectory, we want to define the *reactant segment* and the *product segment* of the trajectory. For this discussion we will limit ourselves to the forward reactive trajectories. The discussion for the reverse reactive trajectories is identical, provided we change the sign of q_n and p_n.

In Fig. 3 we show a forward reactive trajectory as the dashed curve. We consider the initial condition of the trajectory to be in the forward reactive region with initial condition $p_n > 0$ and $q_n < 0$. The trajectory evolves in time until the q_n reaches zero (i.e, the trajectory reaches the transition state) after which the q_n component increases monotonically. The segment of the trajectory with $q_n < 0$ is referred to as the *reactant segment* (shown in Fig. 3 b)) and the segment of the trajectory with $q_n > 0$ is referred to as the *product segment* (shown in Fig. 3 c)).

In Fig. 4 we show the portion of the reactive region corresponding to forward and reverse reactant segments of trajectories.

In Fig. 5 we show the portion of the reactive region corresponding to forward and reverse product segments of trajectories.

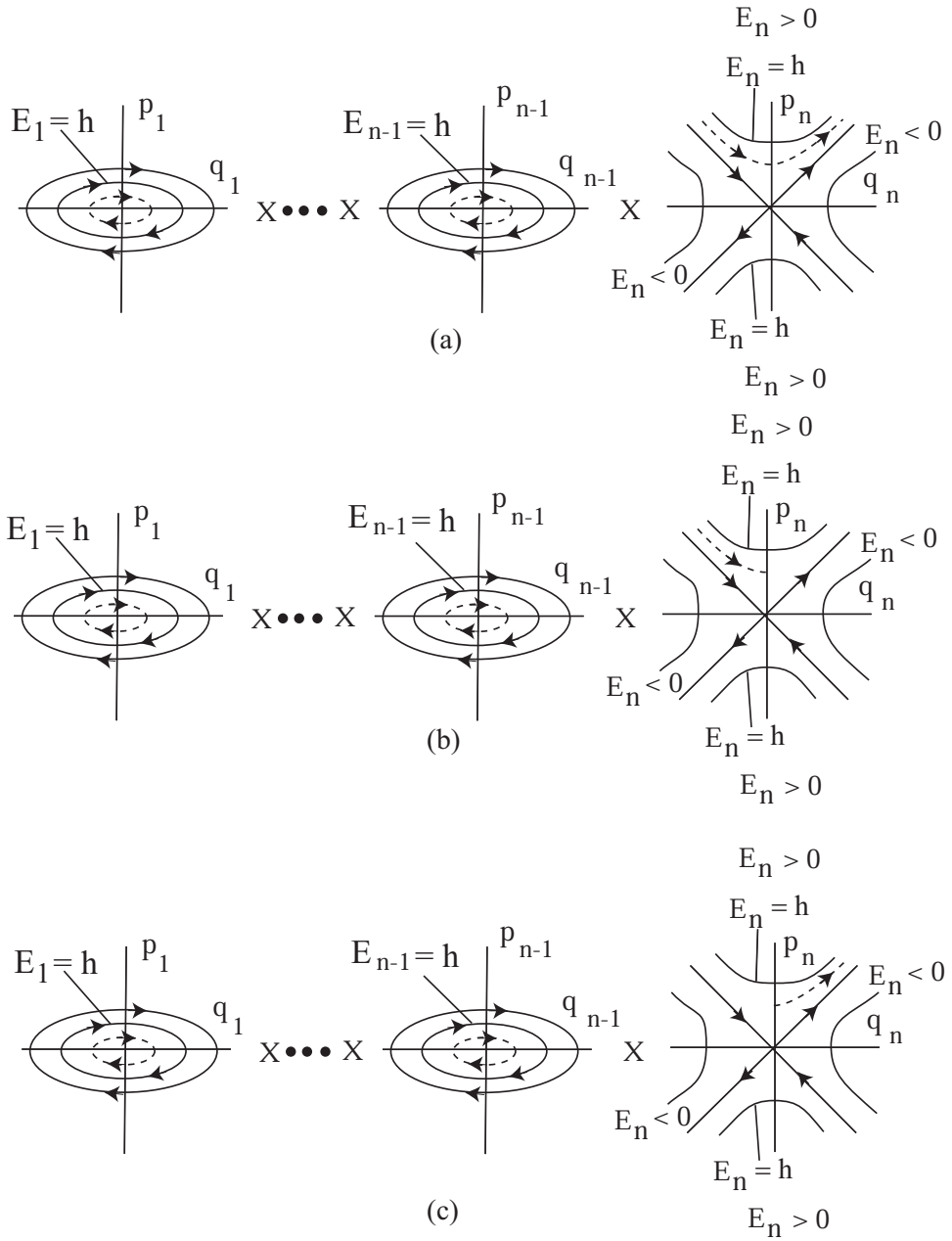

Figure 3: a) A forward reactive trajectory is shown dashed. b) The reactant segment of the foward reactive trajectory. c) The product segment of the forward reactive trajectory. The transition from reactant segment to product segment occurs at the transition state, $q_n = 0$.

2.1.7 The Interior of the Stable and Unstable Spherical Cylinders and the Impenetrable Barriers

Above we described the region bounded by the stable and unstable cylinders and its relation to the reactive trajectories and the transition state. Now we describe the notion of the "interior" of the stable and unstable cylinders. This is a familiar concept from our experience with cylinders in $\mathbb{R}^{2n-1}$. However, these cylinders are in $S^{2n-2} \times \mathbb{R}$.

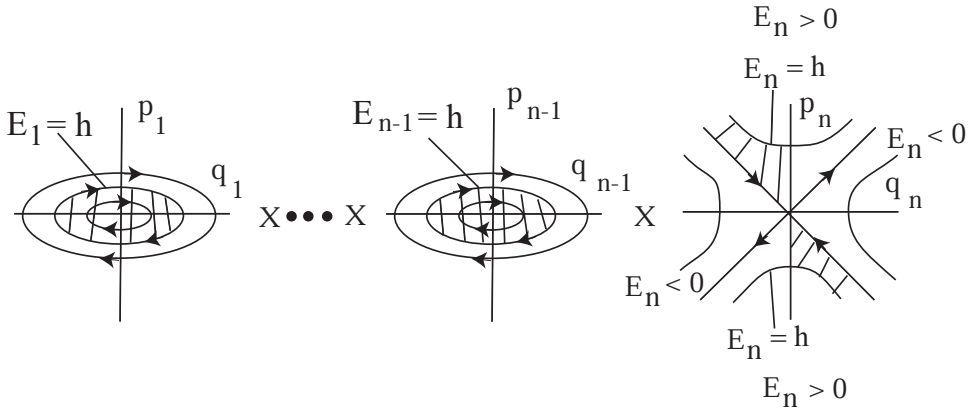

Figure 4: The cross-hatched region corresponds to the portion of the reactive region corresponding to forward and reverse reactant segments.

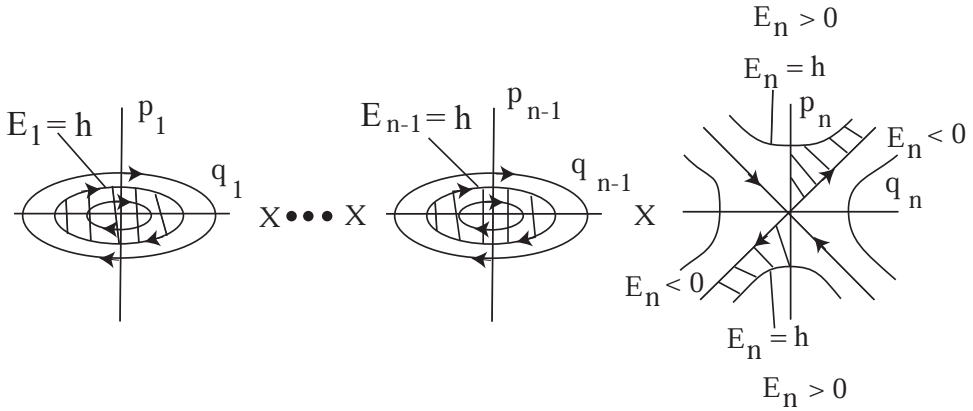

Figure 5: The cross-hatched region corresponds to the portion of the reactive region corresponding to forward and reverse product segments.

Recall that the $2n-2$ dimensional stable spherical cylinder associated with the NHIM is given by:

$$\frac{1}{2}\sum_{i=1}^{n-1}\left(p_i^2+\omega_i^2 q_i^2\right)=h, \quad p_n=-\lambda q_n, \quad \text{stable spherical cylinder.}$$

We consider two "halves" of the stable spherical cylinder. The forward stable spherical cylinder corresponds to $p_n > 0$ and the backward stable spherical cylinder corresponds to $p_n < 0$.

Similarly, the unstable spherical cylinder associated with the NHIM is given by:

$$\frac{1}{2}\sum_{i=1}^{n-1}\left(p_i^2+\omega_i^2 q_i^2\right)=h, \quad p_n=\lambda q_n, \quad \text{unstable spherical cylinder,}$$

with the forward unstable spherical cylinder corresponding to $p_n > 0$ and the backward unstable spherical cylinder corresponding to $p_n < 0$. At $p_n = 0$ the forward and backward stable spherical

cylinders and the forward and backward unstable spherical cylinders are all "glued together" at the transition state $q_n = 0$.

Now one would like to think about the "inside" and "outside" of these spherical cylinders and the nature of the trajectories in these regions.

Mathematically, the spherical cylinder is $S^{2n-3} \times \mathbb{R}$. So what is the "inside" of this object? One way to get inside the cylinder is to imagine how one might put one cylinder inside another. To do this, you would "shrink the radius of S^{2n-3}" and leave $\mathbb{R}$ alone. In other words, we would take:

$$0 < \frac{1}{2} \sum_{i=1}^{n-1} \left(p_i^2 + \omega_i^2 q_i^2 \right) = \sum_{i=1}^{n-1} E_i < h.$$

However, we want all the trajectories inside the spherical cylinder to have the same energy equal to h. This is easy to understand for these n uncoupled linear systems. Since by shrinking the radius of S^{2n-3} we are decreasing the energy in the $q_1 - p_1 \cdots q_{n-1} - p_{n-1}$ component of the trajectory, we must increase the energy in the $q_n - p_n$ component. From Fig. 1 one can see the regions in the $q_n - p_n$ plane with positive energy. Therefore the $q_n - p_n$ component of trajectories in the interior of the spherical cylinders must satisfy:

$$\frac{1}{2} p_n^2 - \frac{1}{2} \lambda^2 q_n^2 = E_n > 0,$$

and we must have

$$\sum_{i=1}^{n} E_i = h.$$

This argument was completely independent of whether we were considering the stable or the unstable spherical cylinder, as well as the forward or backward components of a spherical cylinder. It applies equally to both. Therefore, we see that the *interiors of the stable and unstable spherical cylinders are identical.* That is, *they contain the same trajectories.* Using the terminology developed above, these trajectories are divided into reactive and product segments by the transition state. However, we are forced to the conclusion that the stable and unstable spherical cylinders contain the same trajectories since the only way trajectories can escape the cylinders is by going to infinity as the walls of the spherical cylinders are invariant manifolds (hence, "impenetrable barriers in phase space" [62]).

2.1.8 A Theorem

All of our previous points can be summarized in the following theorem.

Theorem 2.2 *The stable and unstable spherical cylinders bound a region in the energy surface that is divided into two disconnected components by the transition state. All reactive trajectories start inside one connected component, cross the transition state, and leave the transition state passing into the other connected component.*

Several comments are now in order.

- We see that the transition state is the geometrical object separating the reactants from the products in the region bounded by the stable and unstable spherical cylinders.

- The local stable and unstable manifolds of the saddle do not intersect the transition state. Rather, they are the boundaries that define the trajectories that pass through the transition state.
- The stable and unstable spherical cylinders have the same interior.

We now turn to the case where Hamilton's equations are nonlinear.

2.2 Phase Space Structure and the Transition State for a Class of n-Degree-of-Freedom Nonlinear Hamiltonian Systems

Consider a Hamiltonian of the following form:

$$H = \sum_{i=1}^{n-1} \frac{\omega_i}{2}\left(p_i^2 + q_i^2\right) + \lambda q_n p_n + f_1(q_1, \ldots, q_{n-1}, p_1, \ldots, p_{n-1}, \mathcal{I}) + f_2(q_1, \ldots, q_{n-1}, p_1, \ldots, p_{n-1}),$$

$$(q_1, \ldots, q_n, p_1, \ldots, p_n) \in \mathbb{R}^{2n}, \tag{17}$$

where $\mathcal{I} \equiv p_n q_n$ and f_1, f_2 are at least of third order, i.e., they are responsible for the nonlinear terms in the Hamiltonian vector field, and $f_1(q_1, \ldots, q_{n-1}, p_1, \ldots, p_{n-1}, 0) = 0$. Note that the quadratic part of the Hamiltonian (17) is different from the quadratic Hamiltonian (1). Nevertheless, they are equivalent as one can be obtained from another via a linear transformation. The corresponding Hamiltonian vector field is given by:

$$\begin{aligned}
\dot{q}_i &= \frac{\partial H}{\partial p_i} = \omega_i p_i + \frac{\partial f_1}{\partial p_i} + \frac{\partial f_2}{\partial p_i}, \\
\dot{p}_i &= -\frac{\partial H}{\partial q_i} = -\omega_i q_i - \frac{\partial f_1}{\partial q_i} - \frac{\partial f_2}{\partial q_i}, \qquad i = 1, \ldots, n-1, \\
\dot{q}_n &= \frac{\partial H}{\partial p_n} = \lambda q_n + \frac{\partial f_1}{\partial \mathcal{I}} q_n, \\
\dot{p}_n &= -\frac{\partial H}{\partial q_n} = -\lambda p_n - \frac{\partial f_1}{\partial \mathcal{I}} p_n.
\end{aligned} \tag{18}$$

Before we analyze (18) we show that any Hamiltonian vector field in the neighborhood of an equilibrium point of saddle $\times$ center $\times \cdots \times$ center type can be transformed to the form of (17).

2.3 A Normal Form

Normal form theory gives us sufficient conditions for a Hamiltonian to be transformed into the form of (17) in the neighborhood of an equilibrium point of center $\times \cdots \times$ center $\times$ saddle type. This result is well known, see, e.g., [1].

Theorem 2.3 *Consider an arbitrary Hamiltonian vector field. Suppose this vector field has an equilibrium point at which the matrix associated with the linearization has eigenvalues $\pm i\omega_j$, $j = 1, \ldots, n-1$, and $\pm\lambda$. Moreover, we assume that the submatrix corresponding to the imaginary eigenvalues is semisimple (i.e., the complexification is diagonalizable). Then there exists a sequence of local, nonlinear transformations of the coordinates that transforms the Hamiltonian into the form of (17) up to arbitrarily high order.*

Proof: Here we outline the main ideas involved. First we perform a Taylor expansion of the Hamiltonian (17):

$$H = H_2 + H_3 + H_4 + \cdots, \tag{19}$$

where H_k is a homogeneous polynomial of degree k in $q_1 - \cdots - q_n - p_1 - \cdots - p_n$.

The quadratic part of the Hamiltonian, H_2, is given by:

$$H_2 = \sum_{i=1}^{n-1} \frac{\omega_i}{2}(q_i^2 + p_i^2) + \lambda q_n p_n. \tag{20}$$

We then transform the nonhyperbolic part of H_2 into complex coordinates:

$$z_j = q_j + ip_j, \qquad \bar{z}_j = q_j - ip_j, \quad j = 1, \ldots, n-1.$$

In these coordinates H_2 becomes:

$$H_2 = \sum_{j=1}^{n-1} \frac{\omega_j}{2}|z_j|^2 + \lambda q_n p_n. \tag{21}$$

Then in these coordinates H_k is made up of linear combinations of terms of the form:

$$z_1^{k_1} \cdots z_{n-1}^{k_{n-1}} q_n^{k_n} \bar{z}_1^{\ell_1} \cdots \bar{z}_{n-1}^{\ell_{n-1}} p_n^{\ell_n}, \quad \text{where} \quad k_i,\, \ell_i \geq 0, \quad k_1 + \cdots + k_n + \ell_1 + \cdots + \ell_n = k. \tag{22}$$

We need one more piece of notation. The Poisson bracket between two scalar valued functions, F and G, in these variables is given by:

$$\{F, G\} \equiv 2i \sum_{j=1}^{n-1} \left(\frac{\partial F}{\partial \bar{z}_j}\frac{\partial G}{\partial z_j} - \frac{\partial F}{\partial z_j}\frac{\partial G}{\partial \bar{z}_j} \right) + \frac{\partial F}{\partial q_n}\frac{\partial G}{\partial p_n} - \frac{\partial F}{\partial p_n}\frac{\partial G}{\partial q_n}. \tag{23}$$

Now the map

$$\mathrm{ad}_{H_2}(\cdot) \equiv \{\cdot, H_2\}, \tag{24}$$

is a linear map of the space of homogeneous polynomials of degree k into itself. Normal form theory tells us that the only terms that cannot be removed from (19) at order k are those in the kernel of $\mathrm{ad}_{H_2}(\cdot)$. A simple calculation shows that

$$\begin{aligned} &\mathrm{ad}_{H_2}\left(z_1^{k_1} \cdots z_{n-1}^{k_{n-1}} q_n^{k_n} \bar{z}_1^{\ell_1} \cdots \bar{z}_{n-1}^{\ell_{n-1}} p_n^{\ell_n} \right) \\ &\quad = \left(i \sum_{j=1}^{n-1} \omega_j (k_j - \ell_j) + \lambda(\ell_n - k_n) \right) z_1^{k_1} \cdots z_{n-1}^{k_{n-1}} q_n^{k_n} \bar{z}_1^{\ell_1} \cdots \bar{z}_{n-1}^{\ell_{n-1}} p_n^{\ell_n}. \end{aligned} \tag{25}$$

So we see that $z_1^{k_1} \cdots z_{n-1}^{k_{n-1}} q_n^{k_n} \bar{z}_1^{\ell_1} \cdots \bar{z}_{n-1}^{\ell_{n-1}} p_n^{\ell_n}$ is an eigenvector for $\mathrm{ad}_{H_2}(\cdot)$ with eigenvalue $i\sum_{j=1}^{n-1} \omega_j(k_j - \ell_j) + \lambda(\ell_n - k_n)$. Therefore terms of the form (22) cannot be removed if

$$i \sum_{j=1}^{n-1} \omega_j (k_j - \ell_j) + \lambda(\ell_n - k_n) = 0. \tag{26}$$

Now we want to show that a coordinate system exists in which q_n and p_n appear only as a product of each other in the Hamiltonian. This follows immediately from (26) since if that quantity is zero then both the real and imaginary parts must be zero. The real part being zero implies that $k_n = \ell_n$. Therefore, from (22), the power on the q_n and p_n coordinates must be zero at any order. □

Several points should be made concerning this result.

- This argument merely shows that such a coordinate system exists which brings the Hamiltonian into the form of (17) *order by order*. Actually computing this coordinate transformation which would bring an arbitrary Hamiltonian into the form of (17) is a different matter that we will discuss later on.

- It is well known (see, e.g., [1]) that the normal form transformations do not converge in the sense that normalization to all orders generally does not yield a meaningful result. However, this is of no consequence for our purposes. We view the technique more as the input to a numerical method for realizing the NHIM, its stable and unstable manifolds, and the transition state. In this sense the limitations of machine precision make normalization beyond a certain finite order meaningless.

- This is a local result valid in the neighborhood of the equilibrium point of center $\times \cdots \times$ center $\times$ saddle type. However, once the phase space structure is established locally, it can be numerically continued outside of the local region.

- The normalization procedure does not require reversibility, or that the Hamiltonian be of the form kinetic plus potential energy. Indeed, our example of hydrogen in crossed electric and magnetic fields contains significant Coriolis interactions which are neither fully kinetic nor fully potential [54].

- If the $n-1$ frequencies ω_i are nonresonant, then the truncated normal form (at any order) is integrable. That is, the quantities $J_i = \frac{1}{2}\left(p_i^2 + q_i^2\right),\ i = 1, \ldots, n-1$ and $\mathcal{I} = p_n q_n$ are integrals of the truncated normal form and the Hamiltonian can be written as a function of these integrals. In these coordinates the quantity $\frac{\partial f_1}{\partial \mathcal{I}}$ becomes a constant and the $q_n - p_n$ component of Hamilton's equations becomes a simple, one degree-of-freedom saddle.

  Integrable behavior near a saddle has previously been noted in some classical trajectory calculations in the chemical literature, see [22], [40], [31], [24]. Our work gives a rigourous explanation for this behavious, as well as explaining the precise conditions in order for it to occur.

- It may be that we can find a chemical or atomic Hamiltonian a priori in the form of (17). In that case normalization is not required and the setting is global from the start.

- We will show later that the Hamiltonian of a hydrogen atom in crossed electric and magnetic fields can be transformed to the form of (17).

Now we return to the analysis of (18).

2.3.1 Normally Hyperbolic Invariant Manifolds (NHIMs) and their Stable and Unstable Manifolds

The dynamics occurs in the $2n-1$-dimensional energy surface given by:

$$\sum_{i=1}^{n-1} \frac{\omega_i}{2}\left(p_i^2+q_i^2\right) + \lambda q_n p_n + f_1(q_1,\ldots,q_{n-1},p_1,\ldots,p_{n-1},\mathcal{I}) \\ +f_2(q_1,\ldots,q_{n-1},p_1,\ldots,p_{n-1}) = h = constant > 0. \tag{27}$$

Note that if we set $q_n = p_n = 0$ in (18) then $\dot{q}_n = \dot{p}_n = 0$. Therefore $q_n = p_n = 0$ is a $2n-2$ dimensional invariant manifold also for this problem. Its intersection with the $2n-1$-dimensional energy surface, denoted $\mathcal{M}_h^{2n-3}$, is given by

$$\mathcal{M}_h^{2n-3} = \sum_{i=1}^{n-1} \frac{\omega_i}{2}\left(p_i^2+q_i^2\right) + f_2(q_1,\ldots,q_{n-1},p_1,\ldots,p_{n-1}) = h = constant > 0. \tag{28}$$

Regardless of its stability properties, or the size of the nonlinearity, (28) is always an invariant manifold. However, we are interested in the case when it is of the saddle type with stable and unstable manifolds. There are two approaches to this.

- Normally hyperbolic invariant manifolds persist under perturbation. If we are in the setting where the form of (17) must first be obtained by applying normal form theory then we are restricted to a sufficiently small neighborhood of the equilibrium point. In this case the nonlinear terms are much smaller than the linear terms. Therefore, the sphere present in the linear problem becomes a deformed sphere for the nonlinear problem and still has $2n-2$ dimensional stable and unstable manifolds in the $2n-1$ dimensional energy surface since normal hyperbolicity is preserved under perturbations.

- If the Hamiltonian is of the form of (17) then a preliminary, local, transformation is not required. The manifold (28) is invariant regardless of the size of the nonlinearity. Moreover, it is also of saddle type with respect to stability in the transverse directions. This can be seen by examining (18). On $q_n = p_n = 0$ the transverse directions, i.e., q_n and p_n, are still of saddle type (more precisely, they grow and decay exponentially).

Just as for the linear Hamiltonian system discussed earlier, due to their exponentially growing and decaying nature the coordinates $q_n - p_n$ are referred to as the reaction coordinates and the remaining coordinates are referred to as the bath coordinates. In the $q_n - p_n$ phase portrait the trajectories that go from $p_n > q_n > 0$ (resp. $p_n < q_n < 0$) to $q_n > p_n > 0$ (resp. $q_n < p_n < 0$) are said to be the trajectories that undergo reaction, see Fig. 6. (Keep in mind that for nonlinear Hamiltonian systems this is a local picture valid near (28), i.e., $q_n = p_n = 0$.) These are the trajectories with $q_n p_n > 0$ in Fig. 6. We can see from Fig. 6 that there are two types of *reactive trajectories*. Those with q_n, $p_n > 0$, which are referred to as the *forward reactive trajectories* and those with q_n, $p_n < 0$ which are referred to as the *backward reactive trajectories*. Notice that the q_n and p_n components of a reactive trajectory cannot change sign during their evolution. The trajectories with $q_n p_n < 0$ are referred to as *nonreactive trajectories*.

A key advantage of the normal form is that the stable and unstable manifolds of $\mathcal{M}_h^{2n-3}$ are known explicitly. They are given by:

$$W^s\left(\mathcal{M}_h^{2n-3}\right) = \left\{(q_1,\ldots,q_n,p_1,\ldots,p_n) \,|\, \sum_{i=1}^{n-1} \frac{\omega_i}{2}\left(p_i^2+q_i^2\right) \right. \\ \left. +f_2(q_1,\ldots,q_{n-1},p_1,\ldots,p_{n-1}) = h = constant > 0,\ q_n = 0\right\},$$

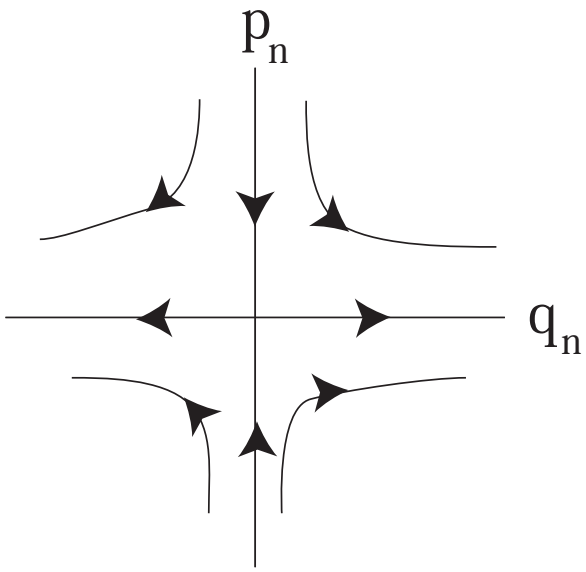

Figure 6: The projection of the reacting trajectories into the $q_n - p_n$ plane near $q_n = p_n = 0$.

$$W^u\left(\mathcal{M}_h^{2n-3}\right) = \left\{(q_1,\ldots,q_n,p_1,\ldots,p_n)\,|\,\sum_{i=1}^{n-1}\frac{\omega_i}{2}\left(p_i^2+q_i^2\right)\right.$$
$$\left.+f_2(q_1,\ldots,q_{n-1},p_1,\ldots,p_{n-1}) = h = constant > 0,\ p_n = 0\right\}. \quad (29)$$

Hence, the stable and unstable manifolds of the sphere have the structure of $\mathcal{M}_h^{2n-3} \times \mathbb{R}$.

In the language of dynamical systems theory both the stable and unstable cylinders have two "branches" corresponding to $p_n > 0$ and $p_n < 0$. In the language of reaction dynamics we will see that these two branches are related to the forward and backward reactions. Consequently, it is useful to develop a notation for the two branches of the stable and unstable cylinders. Accordingly, we make the following definitions.

The forward stable manifold of $\mathcal{M}_h^{2n-3}$:

$$W_f^s\left(\mathcal{M}_h^{2n-3}\right) = \left\{(q_1,\ldots,q_n,p_1,\ldots,p_n)\,|\,\sum_{i=1}^{n-1}\frac{\omega_i}{2}\left(p_i^2+q_i^2\right)\right.$$
$$\left.+f_2(q_1,\ldots,q_{n-1},p_1,\ldots,p_{n-1}) = h = constant > 0,\ q_n = 0,\ p_n > 0\right\}. \quad (30)$$

The backward stable manifold of $\mathcal{M}_h^{2n-3}$:

$$W_b^s\left(\mathcal{M}_h^{2n-3}\right) = \left\{(q_1,\ldots,q_n,p_1,\ldots,p_n)\,|\,\sum_{i=1}^{n-1}\frac{\omega_i}{2}\left(p_i^2+q_i^2\right)\right.$$
$$\left.+f_2(q_1,\ldots,q_{n-1},p_1,\ldots,p_{n-1}) = h = constant > 0,\ q_n = 0,\ p_n < 0\right\}. \quad (31)$$

The forward unstable manifold of $\mathcal{M}_h^{2n-3}$:

$$W_f^u\left(\mathcal{M}_h^{2n-3}\right) = \left\{(q_1,\ldots,q_n,p_1,\ldots,p_n)\,|\,\sum_{i=1}^{n-1}\frac{\omega_i}{2}\left(p_i^2+q_i^2\right)\right.$$
$$\left.+f_2(q_1,\ldots,q_{n-1},p_1,\ldots,p_{n-1}) = h = constant > 0,\ p_n = 0,\ q_n > 0\right\}. \tag{32}$$

The backward unstable manifold of $\mathcal{M}_h^{2n-3}$:

$$W_b^u\left(\mathcal{M}_h^{2n-3}\right) = \left\{(q_1,\ldots,q_n,p_1,\ldots,p_n)\,|\,\sum_{i=1}^{n-1}\frac{\omega_i}{2}\left(p_i^2+q_i^2\right)\right.$$
$$\left.+f_2(q_1,\ldots,q_{n-1},p_1,\ldots,p_{n-1}) = h = constant > 0,\ p_n = 0,\ q_n < 0\right\}. \tag{33}$$

The stable and unstable manifolds of $\mathcal{M}_h^{2n-3}$ are the natural higher-dimensional analogs of the 2dof "cylinder manifolds" described in Ref. [42].

2.3.2 The Relation of the Normally Hyperbolic Invariant Manifolds to the Center Manifold of the Origin

The Hamiltonian vector field (18) has an equilibrium point at the origin which has a $2n-2$ dimensional center manifold given by $p_n = q_n = 0$, a one-dimensional stable manifold given by $q_i = p_i = 0$, $i = 1,\ldots,n-1$, $q_n = 0$, and a one-dimensional unstable manifold given by $q_i = p_i = 0$, $i = 1,\ldots,n-1$, $p_n = 0$. It is easy to check that the stable and unstable manifolds of the origin have the same energy as the origin, i.e., $h = 0$. We say that they are *isoenergetic*. However, the center manifold of the origin is not isoenergetic. The intersection of the center manifold of the origin with the energy surface is given by:

$$\frac{1}{2}\sum_{i=1}^{n-1}p_i^2 + \frac{1}{2}\sum_{i=1}^{n-1}\omega_i^2 q_i^2 + f_2(q_1,\ldots,q_{n-1},p_1,\ldots,p_{n-1}) = h = constant.$$

This is the normally hyperbolic invariant $2n-3$ dimensional manifold we described earlier. Hence we see that the center manifold of the origin is foliated by a one-parameter (the energy) family of normally hyperbolic invariant $2n-3$ dimensional manifolds.

2.4 The Transition State

Now we construct the transition state. This is obtained by setting $q_n = p_n$. On the energy surface this gives:

$$\sum_{i=1}^{n-1}\frac{\omega_i}{2}\left(p_i^2+q_i^2\right) + \lambda p_n^2 + f_1(q_1,\ldots,q_{n-1},p_1,\ldots,p_{n-1},p_n^2)$$
$$+f_2(q_1,\ldots,q_{n-1},p_1,\ldots,p_{n-1}) = h = constant. \tag{34}$$

This is a $2n-2$-dimensional surface that is divided into two halves; $p_n > 0$ and $p_n < 0$. The surface is divided into these two halves by $p_n = 0$, which corresponds to the invariant manifold $\mathcal{M}_h^{2n-3}$,

which again plays a role analogous to the PODS. If we are close to the equilibrium point so that the nonlinearity is small, then the transition state is a deformed $2n-2$-dimensional sphere. Now we prove that (34) is *locally* a surface of no return for the trajectories of Hamilton's equations given in (18). What "locally" means is that there is a neighborhood of (34) that trajectories starting on (34) (except those starting on the $2n-3$ dimensional invariant manifold (28)) must leave before they can possibly re-intersect (34).

Theorem 2.4 *The $2n-2$ dimensional invariant manifold given in (34) is a surface of no return for the trajectories of Hamilton's equations given in (18),* except *for trajectories starting on the invariant $2n-3$ dimensional manifold given in (28).*

Proof: The $2n-2$ dimensional invariant manifold in the energy surface is defined by $q_n = p_n$. If we examine Hamilton's equations (18) we see that the vector field is not tangent to (34). Moreover, the vector field is not zero on (34). Therefore trajectories starting on (34) always leave (34). By continuity of solutions with respect to initial conditions they must leave a neighborhood of (34) before possibly returning. □

Now we turn to describing the nature of the stable and unstable manifolds in relation to the transition state.

Theorem 2.5 *The $2n-2$ dimensional $W^s\left(\mathcal{M}_h^{2n-3}\right)$ and $W^u\left(\mathcal{M}_h^{2n-3}\right)$ bound a region in the $2n-1$ dimensional energy surface that is divided into two components by the transition state. All reacting trajectories start in one component, cross the transition state, then enter the other component.*

Proof: We work on a fixed energy surface with energy value $h = constant > 0$.

The reactant segments of the forward reactive trajectories are contained in the region:

$$0 < \sum_{i=1}^{n-1} \frac{\omega_i}{2}\left(p_i^2 + q_i^2\right) + f_2(q_1, \ldots, q_{n-1}, p_1, \ldots, p_{n-1}) < h, \qquad p_n > q_n > 0, \tag{35}$$

and the reactant segments of the backward reactive trajectories are contained in the region:

$$0 < \sum_{i=1}^{n-1} \frac{\omega_i}{2}\left(p_i^2 + q_i^2\right) + f_2(q_1, \ldots, q_{n-1}, p_1, \ldots, p_{n-1}) < h, \qquad p_n < q_n < 0. \tag{36}$$

In figure 7 we illustrate a forward and backward reacting trajectory.
In Fig. 8 we illustrate just the reactant segment of the forward and backward reacting trajectory shown in Fig. 7.

The product segments of the forward reactive trajectories are contained in the region:

$$0 < \sum_{i=1}^{n-1} \frac{\omega_i}{2}\left(p_i^2 + q_i^2\right) + f_2(q_1, \ldots, q_{n-1}, p_1, \ldots, p_{n-1}) < h, \qquad 0 < p_n < q_n, \tag{37}$$

and the product segments of the backward reactive trajectories are contained in the region:

$$0 < \sum_{i=1}^{n-1} \frac{\omega_i}{2}\left(p_i^2 + q_i^2\right) + f_2(q_1, \ldots, q_{n-1}, p_1, \ldots, p_{n-1}) < h, \qquad 0 > p_n > q_n. \tag{38}$$

In Fig. 9 we illustrate the product segments of the forward and backward reacting trajectory shown in Fig. 7.

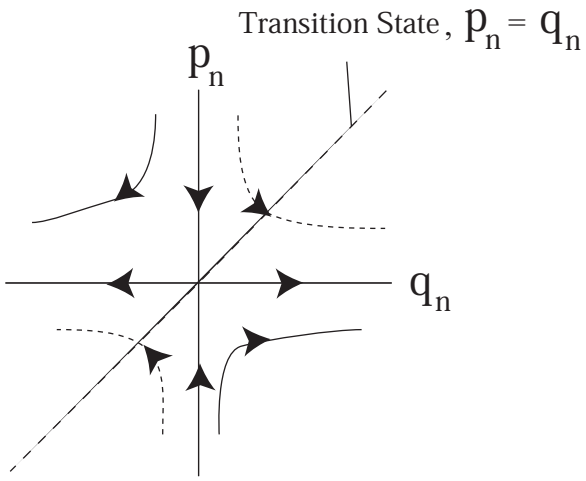

Figure 7: The projection of a forward and backward reacting trajectory into the $q_n - p_n$ plane.

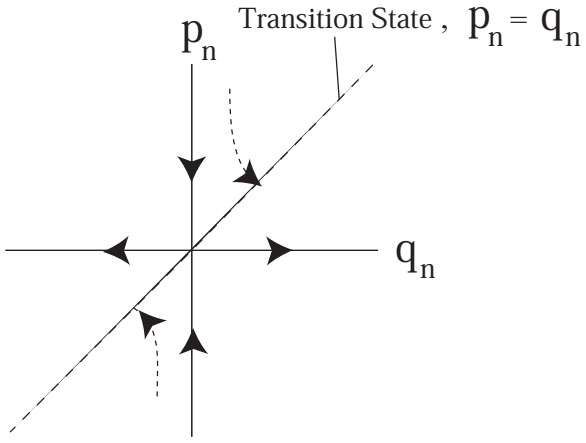

Figure 8: The projection of the reactant segment of the forward and backward reacting trajectory shown in Fig. 7 into the $q_n - p_n$ plane.

Now consider a forward reacting trajectory (i.e., $p_n > q_n > 0$). It follows by examining the $q_n - p_n$ phase portrait in Fig. 7 that the p_n component of the trajectory decreases. It reaches the line $q_n = p_n$, at which point it has reached the transition state as defined in (34). It then crosses the transition state. □

2.5 Search Algorithm for the Transition State

Before applying the theory developed in this section to the ionization of the hydrogen atom in crossed electric and magnetic fields we summarize the steps developed above.

1. For a given Hamiltonian, find an equilibrium point for which the eigenvalues of the matrix associated with the linearization about the equilibrium point have the form described in (17).

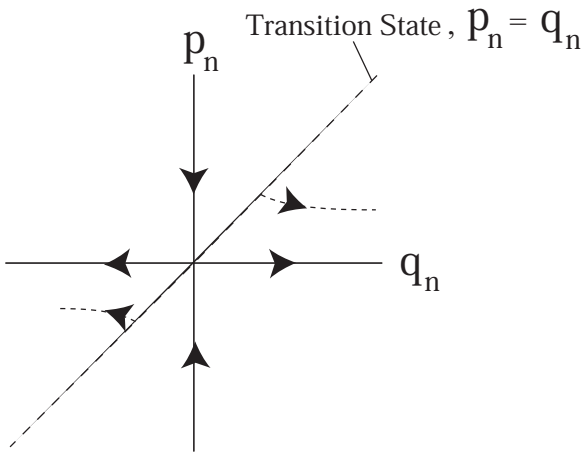

Figure 9: The projection of the product segment of the forward and backward reacting trajectories shown in Fig. 7 into the $q_n - p_n$ plane.

2. Transform the Hamiltonian to the normal form described above up to the desired degree of accuracy using a symbolic manipulator. The Hamiltonian is now in a new coordinate system that we will call the "normal form coordinates".

3. Our arguments above show how to identify the transition state (34) and the higher dimensional analogs of the stable and unstable manifolds that mediate the reaction in the normal form coordinates.

4. These structures can be visualized in the original coordinates by using the inverse of the normal form transformation, which is computed symbolically along with the normal form transformation.

5. Integrals of flux across the transition state can be computed in the normal form coordinates since the transformation between the original coordinates and the normal form coordinates is symplectic, hence volume preserving.

2.6 Flux Through the Transition State

We now discuss the issue of flux through the transition state, and derive a simple form for it which follows from the normal form for Hamilton's equations described in Theorem 2.3. The abstract flux formulae we use are taken from [34], whose formalism we follow. The flux through the transition state is important in reaction dynamics since the reaction rate can be obtained by dividing this flux by the appropriate partition function [44].

We begin with some formalism. Consider the phase space $\mathbb{R}^{2n}$ with the canonical symplectic 2-form:

$$\omega = dp_1 \wedge dq_1 \wedge \cdots \wedge dp_n \wedge dq_n. \tag{39}$$

We consider the volume $2n$-form on $\mathbb{R}^{2n}$ defined by:

$$\Omega = \frac{1}{n!}\omega^n. \tag{40}$$

We define the following $(2n-2)$-form by:

$$\Omega' = \frac{1}{(n-1)!}\omega^{n-1}. \tag{41}$$

Let λ be a $(2n-3)$-form such that:

$$d\lambda = \Omega'. \tag{42}$$

We refer to the *forward transition state* as the component of the transition state given by $p_n > 0$, and the *backward transition state* as the component of the transition state given by $p_n < 0$. These two components of the transition state are separated by the NHIM. Then the following result (which we state in the context of our set-up) is proven in [34].

Theorem 2.6 (MacKay, 1990) *The flux of energy surface volume across the forward transition state in the energy surface $H = h =$ constant is given by:*

$$\int_{NHIM} \lambda. \tag{43}$$

The flux across the backward transition state is given by the negative of this result.

Furthermore, it is shown in [34] that if one neglects the nonlinear terms in the Hamiltonian vector field, we have:

$$\int_{S^{2n-3}} \lambda = \frac{h^{n-1}}{(n-1)!} \prod_{i=1}^{n-1} \frac{2\pi}{\omega_i}. \tag{44}$$

The normal form techniques allow us to go further and compute the nonlinear corrections to this formula, to as high an order as we compute the normal form. In the case where the $n-1$ frequencies associated with the bath coordinates are incommensurate, then we get a very simple formula for the flux across the transition state, and it is only this case that we consider here as it is the situation for the Rydberg atom in crossed fields that we consider in the next section.

Let $J_1, \ldots, J_{n-1}, \mathcal{I}$ denote the n approximate integrals of the normal form. Let $\theta_1, \ldots, \theta_{n-1}, \theta_n$ denote the associated canonical coordinates, the first $n-1$ of which are angles. Note that the NHIM is given by $\mathcal{I} = 0$.

If we now take the canonical symplectic form to be:

$$\tilde{\omega} = dJ_1 \wedge d\theta_1 \wedge \cdots \wedge dJ_{n-1} \wedge d\theta_{n-1} \wedge d\mathcal{I} \wedge d\theta_n, \tag{45}$$

then we have

$$\tilde{\lambda} = J_1 d\theta_1 \wedge dJ_2 \wedge d\theta_2 \cdots \wedge dJ_{n-1} \wedge d\theta_{n-1} + (n-1) \text{ similar terms.} \tag{46}$$

Since $\mathcal{I} = 0$ on the NHIM, the only term that contributes to the integral:

$$\int_{NHIM} \tilde{\lambda},$$

is the first term. Hence, the flux across the forward transition state is given by:

$$\int_{NHIM} \tilde{\lambda} = (2\pi)^{n-1} \prod_{i=1}^{n-1} J_i. \tag{47}$$

The flux across the backward transition state is the negative of this value. It is interesting that the flux is represented completely in terms of the approximate integrals of motion associated with the "bath modes".

3 Application to the Hydrogen Atom in Crossed Electric and Magnetic Fields

The ionization of a hydrogen atom interacting with combinations of external electric and magnetic fields is an intricate problem of fundamental importance [54], [56], [36], [58], [48], [49]. In this section we use the theory developed above to understand this process.

The problem of ionization of a hydrogen atom in crossed magnetic and electric fields resembles a chemical reaction: in a typical unimolecular reaction [16] the molecule is first "activated" by the injection of sufficient energy so that it can overcome the barrier to reaction. Some time after the activation, if energy finds its way into the reactive mode, the reaction occurs. In the problem of the ionization of hydrogen atoms the "activation" is the initial excitation to a state of very high principal quantum number ($n \sim 50$ or larger). Following state preparation, energy flows into the ionization channel and the electron is detached. In both systems a central question concerns the rate at which the energy migrates into the reactive (or ionizing) mode. In this section we develop an approach to the ionization of hydrogen atoms in crossed electric and magnetic fields that builds on the advances in the theory of chemical reaction dynamics developed in previous sections. The key to describing a chemical reaction is the recognition of the importance of classical phase space structures that govern the progress of the reaction [60]. The theory developed in this article makes these structures explicit for this intricate 3 dof problem.

3.1 Rydberg Atoms

In the past few years innovative, sophisticated experimental techniques have led to renewed interest in atoms or molecules in which one of the electrons is promoted to a high energy state, where it is only weakly bound to the core and its dynamics is approximately hydrogenic [5]. These states are typically characterized by very large principal quantum numbers [19], [23], and such atoms (or molecules) are generically known as "Rydberg" atoms, because the energy levels of the excited electron are well described by a Rydberg-like formula [19]. More precisely, deviations from the pure hydrogenic eigenenergies are induced by the interaction between the Rydberg electron and the electronic cloud around the atomic or molecular core. These deviations are described by the *quantum defect* δ_ℓ, which enters in the formula for the energy levels as a correction to the principal quantum number n [19], [17].

Rydberg atoms and molecules occupy a special place in the physical sciences, as their loosely bound electron lives in that poorly charted territory where the quantum world of the atom transforms into the classical reality of macroscopic objects. Rydberg atoms have many exaggerated properties such as huge dipole moments, and they constitute very convenient, natural laboratory for the investigation of many physical phenomena which they display with exceptional clarity. In these atoms, the Rydberg electron is very weakly bound, and it resides mostly at an immense distance from the atomic or molecular core, to the point that if the Rydberg atoms were solid, they would be just about visible to the naked eye. Laboratory-scale external fields, and even weak stray electric fields [2], become comparable to the atomic, (or molecular) Coulomb field sensed by the Rydberg electron, and interesting dynamical properties, such as, for example, quantum chaology [11], [21], [20], can be studied experimentally.

Rydberg atoms in strong external fields constitute fundamental physical systems where the quantum mechanical regime of strong nonlinearity can be tested [20], [32]. While the problem of a Rydberg atom interacting with a strong magnetic field (the quadratic Zeeman effect, QZE) has been fairly well understood as a result of sustained research in the past two decades [21], [18], the superficially similar scenario resulting from the addition of a perpendicular electric field – the

so-called crossed field arrangement [51], [4], [59], [47], [57], [58] – remains the least understood of all Rydberg problems. In spite of the prominence of the crossed fields in diverse areas of physics ranging from excitonic systems to plasmas and neutron stars. This problem is so complex because no continuous symmetry survives the extensive symmetry breaking [8] induced by the two fields. It has also been found that a velocity-dependent, Coriolis-like force in Newton's equations causes the ionization of the electron to exhibit chaotic scattering [35], [55]. All these phenomena, as well as renewed interest in the motional Stark effect [28], [15], make the crossed fields problem an experimental accessible paradigm for a wide variety of outstanding issues in atomic and molecular physics, solid-state physics [10], [50], nuclear physics [3], astrophysics [38], and celestial mechanics [39].

More recent experiments [49] showed that the ionization threshold has a nontrivial progression with respect to the external fields. Its classical-like scaling behavior (i.e., the progression was found to depend on the scaled fields alone) [49] suggested the possibility of a classical explanation. Recently this classical mechanism [55] which explains and consolidates these findings for energies below, at, and above threshold was documented by showing that the atom undergoes its transition to chaotic scattering due to the existence of a critical point in the Hamiltonian flow. This was done on a reduced dimensionality model which restricted the electron to the plane perpendicular to the magnetic field. The theory developed in preceding sections makes the full 3 dof treatment possible.

3.2 The Hamiltonian and its Normal Form

The Hamiltonian in atomic units ($e = \hbar = m_e = 1$) for the hydrogen atom in crossed electric and magnetic fields in Cartesian coordinates is given by:

$$H = \frac{1}{2}\,(P_1^2 + P_2^2 + P_3^2) - \frac{1}{R} + \left[\frac{\omega_c}{2}\,(x_1\,P_2 - x_2\,P_1) + \frac{\omega_c^2}{8}(x_1^2 + x_2^2) - \epsilon x_1\right], \tag{48}$$

where $R = \sqrt{x_1^2 + x_2^2 + x_3^2}$, ω_c is the cyclotron frequency in atomic units of 2.35×10^5 Tesla and ϵ is the electric field in atomic units of 5.14×10^{11} V/m [54].

Scaling the coordinates by ω_c:

$$\begin{aligned} x_i' &= \omega_c^{2/3}\,x_i, \\ P_i' &= \omega_c^{-1/3}\,P_i, \quad i = 1, 2, 3, \end{aligned} \tag{49}$$

and dropping the primes in order not to complicate the notation, the Hamiltonian becomes:

$$\mathcal{H} = \frac{1}{2}\,(P_1^2 + P_2^2 + P_3^2) - \frac{1}{R} + \left[\frac{1}{2}\,(x_1\,P_2 - x_2\,P_1) + \frac{1}{8}\,(x_1^2 + x_2^2) - \varepsilon\,x_1\right], \tag{50}$$

where $\mathcal{H} = \omega_c^{-2/3} H$ is the scaled energy and $\varepsilon = \omega_c^{-4/3}\,\epsilon$ is the scaled electric field. We adopt the experimentally interesting value of $\varepsilon = 0.58$ in our calculations.

The Hamiltonian $\mathcal{H}$ generates the vector field:

$$\dot{x}_1 = \frac{\partial \mathcal{H}}{\partial P_1} = P_1 - \frac{1}{2}\,x_2,$$

$$
\begin{aligned}
\dot{x}_2 &= \frac{\partial \mathcal{H}}{\partial P_2} = P_2 + \frac{1}{2}\, x_1, \\
\dot{x}_3 &= \frac{\partial \mathcal{H}}{\partial P_3} = P_3, \\
\dot{P}_1 &= -\frac{\partial \mathcal{H}}{\partial x_1} = -\frac{1}{R^3}\, x_1 - \frac{1}{2}\, P_2 - \frac{1}{4}\, x_1 + \varepsilon, \\
\dot{P}_2 &= -\frac{\partial \mathcal{H}}{\partial x_2} = -\frac{1}{R^3}\, x_2 + \frac{1}{2}\, P_1 - \frac{1}{4}\, x_2, \\
\dot{P}_3 &= -\frac{\partial \mathcal{H}}{\partial x_3} = -\frac{1}{R^3}\, x_3.
\end{aligned} \tag{51}
$$

The equilibrium point of interest for this vector field is:

$$
X_0 = (x_1, x_2, x_3, P_1, P_2, P_3) = (\varepsilon^{-1/2}, 0, 0, 0, -\frac{1}{2}\varepsilon^{-1/2}, 0). \tag{52}
$$

We translate the fixed point to the origin via the following coordinate shift:

$$
\hat{x}_1 = x_1 - \varepsilon^{-1/2}, \quad \hat{x}_2 = x_2, \quad \hat{x}_3 = x_3, \quad \hat{P}_1 = P_1, \quad \hat{P}_2 = P_2 + \frac{1}{2}\,\varepsilon^{-1/2}, \quad \hat{P}_3 = P_3. \tag{53}
$$

The new Hamiltonian is then given by:

$$
H \;=\; \frac{1}{2}\,(\hat{P}_1^2 + \hat{P}_2^2 + \hat{P}_3^2) - \frac{1}{\mathcal{R}} + \frac{1}{2}\,(\hat{x}_1\hat{P}_2 - \hat{x}_2\hat{P}_1) + \frac{1}{8}\,(\hat{x}_1^2 + \hat{x}_2^2) - \varepsilon\,\hat{x}_1 - \varepsilon^{1/2}, \tag{54}
$$

where $\mathcal{R} = ((\hat{x}_1 - x_s)^2 + \hat{x}_2^2 + \hat{x}_3^2)^{1/2}$ and $x_s = -\varepsilon^{-1/2}$. From this point on we drop the hats from the variables with the understanding that our equilibrium point has been translated to the origin.

In order to compute the normal form up to a finite order N we will need the Taylor expansion of the Hamiltonian about the origin up through this order:

$$
H' = H + 2\varepsilon^{\frac{1}{2}} = \sum_{n=2}^{N} H_n, \tag{55}
$$

where H_n denotes a homogeneous polynomial in six variables of degree n. We begin by making a Taylor expansion of the term $1/\mathcal{R}$ in the three position variables around the origin up to eighth degree, because the normalization procedure will be pushed up to sixth order, which involves polynomial terms of eighth degree. The terms of the development of $1/\mathcal{R}$ which contribute to the main part of the Hamiltonian are the ones up to second order:

$$
\frac{1}{\mathcal{R}} = \sqrt{\varepsilon} - \varepsilon\, x_1 + \varepsilon^{3/2}\, x_1^2 - \frac{1}{2}\,\varepsilon^{3/2}\,(x_2^2 + x_3^2) + \mathcal{O}(x_i^3), \qquad i = 1, 2, 3. \tag{56}
$$

Since the origin is an equilibrium point the first order terms of the expansion of the Hamiltonian vanish. The constant term is irrelevant to the dynamics. The first relevant terms are the second order terms, which are:

$$
H_2 = \frac{1}{2}\,(P_1^2 + P_2^2 + P_3^2) + \frac{1}{2}\,(x_1 P_2 - x_2 P_1) + \left(\frac{1}{8} - \varepsilon^{3/2}\right)\, x_1^2 + \left(\frac{1}{8} + \frac{1}{2}\,\varepsilon^{3/2}\right)\, x_2^2 + \frac{1}{2}\,\varepsilon^{3/2}\, x_3^2. \tag{57}
$$

3.2.1 Transformation of the Linear Part of Hamilton's Equations

We now construct a change of variables to reduce the Hamiltonian (57) to its real normal form:

$$H_2 = 2\,\eta\,\tilde{x}_1\,\tilde{P}_1 + \nu_1\,(\tilde{x}_2^2 + \tilde{P}_2^2) + \nu_2\,(\tilde{x}_3^2 + \tilde{P}_3^2). \tag{58}$$

Let I_3 be the 3×3 identity matrix and

$$J = \begin{pmatrix} 0 & I_3 \\ -I_3 & 0 \end{pmatrix}. \tag{59}$$

We compute $L = J\,Hess(H_2)$:

$$L = \begin{pmatrix} 0 & -\frac{1}{2} & 0 & 1 & 0 & 0 \\ \frac{1}{2} & 0 & 0 & 0 & 1 & 0 \\ 0 & 0 & 0 & 0 & 0 & 1 \\ -\frac{1}{4} + 2\varepsilon^{3/2} & 0 & 0 & 0 & -\frac{1}{2} & 0 \\ 0 & -\frac{1}{4} - \varepsilon^{3/2} & 0 & \frac{1}{2} & 0 & 0 \\ 0 & 0 & -\varepsilon^{3/2} & 0 & 0 & 0 \end{pmatrix}. \tag{60}$$

The order of the coordinates in this matrix is $x_1, x_2, x_3, P_1, P_2, P_3$. The eigenvalues of L are as follows:

$$\begin{aligned} \lambda_{1,2} &= \pm\frac{i}{\sqrt{2}}\sqrt{1 - \varepsilon^{3/2} + \sqrt{1 - 2\,\varepsilon^{3/2} + 9\,\varepsilon^3}} = \pm\imath\,\nu_1, \\ \lambda_{3,4} &= \pm\frac{1}{\sqrt{2}}\sqrt{-1 + \varepsilon^{3/2} + \sqrt{1 - 2\,\varepsilon^{3/2} + 9\,\varepsilon^3}} = \pm\eta, \\ \lambda_{5,6} &= \pm\imath\,\varepsilon^{3/4} = \pm\imath\,\nu_2, \end{aligned} \tag{61}$$

where $\nu_1, \nu_2, \eta \in \mathbb{R}^+$.

The eigenvectors of L are given by:

$$V(\lambda_i)^T = (\lambda_i, 2\varepsilon^{3/2} - \lambda_i^2, 0, \frac{\lambda_i^2}{2} + \varepsilon^{3/2}, -\lambda_i^3 + \left(-\frac{1}{2} + 2\varepsilon^{3/2}\right)\lambda_i, 0), \quad i = 1, \ldots, 4, \tag{62}$$

and

$$V(\lambda_i)^T = (0, 0, 1/\sqrt{\nu_2}, 0, 0, \pm\imath\sqrt{\nu_2}), \quad i = 5, 6. \tag{63}$$

Now we consider the change of variables:

$$C = (V(-\eta)\,d_1, \Im(V(-\imath\,\nu_1))\,d_2, \Im(V(-\imath\,\nu_2))\,d_3, V(\eta)\,d_4, \Re(V(-\imath\,\nu_1))\,d_5, \Re(V(-\imath\,\nu_2))\,d_6), \tag{64}$$

where $d_i \in \mathbb{C}$, $i = 1, \ldots, 6$ have to be chosen appropriately in order to obtain a canonical transformation to get (58). The condition for the transformation to be symplectic is $C^T\,J\,C = \alpha\,J$, with $\alpha \in \mathbb{C}$. Imposing this condition we obtain that:

$$d_4 = d_1,\ d_5 = d_2\,\alpha,\ d_6 = d_3\,\alpha, \tag{65}$$

and

$$d_1^2 = \alpha/(2\,\eta\,(\eta^4 - 2\,(1+2\,\eta^2)\,\nu_2^2 + 4\,\nu_2^4)),\ d_2^2 = 1/(\nu_1\,(\nu_1^4 - 2\,(1-2\,\nu_1^2)\,\nu_2^2 + 4\,\nu_2^4)),\ d_3^2 = 1,\ \alpha = -1. \tag{66}$$

Hence, by performing the real symplectic change of variables:

$$(x_1, x_2, x_3, P_1, P_2, P_3) = C\,(\tilde{x}_1, \tilde{x}_2, \tilde{x}_3, \tilde{P}_1, \tilde{P}_2, \tilde{P}_3), \tag{67}$$

we obtain the real normal form associated to (57):

$$H_2 = 2\,\eta\,\tilde{x}_1\,\tilde{P}_1 + \nu_1\,(\tilde{x}_2^2 + \tilde{P}_2^2) + \nu_2\,(\tilde{x}_3^2 + \tilde{P}_3^2). \tag{68}$$

Observe that if we had taken $\alpha = 1$ in the construction of the latter change then the resulting Hamiltonian would have been:

$$H_2 = -2\,\eta\,\tilde{x}_1\,\tilde{P}_1 + \nu_1\,(\tilde{x}_2^2 + \tilde{P}_2^2) + \nu_2\,(\tilde{x}_3^2 + \tilde{P}_3^2). \tag{69}$$

In order to obtain the complex normal form associated to (57) we apply the complexifying change:

$$\begin{aligned} \tilde{x}_1 &= q_3, \quad \tilde{x}_2 = \tfrac{q_2 + \imath\,p_2}{\sqrt{2}}, \quad \tilde{x}_3 = \tfrac{q_1 + \imath\,p_1}{\sqrt{2}} \\ \tilde{P}_1 &= p_3, \quad \tilde{P}_2 = \tfrac{\imath\,q_2 + p_2}{\sqrt{2}}, \quad \tilde{P}_3 = \tfrac{\imath\,q_1 + p_1}{\sqrt{2}}, \end{aligned} \tag{70}$$

which leads to the new Hamiltonian:

$$H_2 = \imath\,\omega_1\,q_1\,p_1 + \imath\,\omega_2\,q_2\,p_2 + \mu\,q_3\,p_3, \tag{71}$$

after making the identification $\mu = 2\,\eta$, $\omega_2 = 2\,\nu_1$ and $\omega_1 = 2\,\nu_2$ (note that the reaction coordinate is "3" now). Hence, the nonlinear terms included in H_i, $i > 2$ must be transformed adequately following the same steps used to calculate (71).

The next step is the calculation of the normal form. We plan to reach sixth order in the normalization procedure, which means that the normal form will be an eighth–degree polynomial in $q = (q_1, q_2, q_3)$ and $p = (p_1, p_2, p_3)$. Therefore we have to calculate terms in the Taylor development of $1/\mathcal{R}$ up to degree eight before normalizing. We start by describing the process we shall perform.

3.3 Normalization by Lie Transformations

3.3.1 Lie transformations

The aim of Lie transformations in Hamiltonian theory is to generate a symplectic change of variables depending on a small parameter as the general solution of a Hamiltonian system of differential equations. The method was first proposed by Deprit [9] (we follow the presentation in [43]) and can be stated as follows.

An analytic Hamiltonian function depending on a small parameter σ

$$\mathcal{H}(x;\sigma) \;=\; \sum_{i=0}^{\infty} \frac{\sigma^i}{i!}\,\mathcal{H}_i(x),$$

where Hamiltonians $\mathcal{H}_i(x)$ are analytic functions in x, is transformed into another Hamiltonian

$$\mathcal{K}(y;\sigma) \;=\; \sum_{i=0}^{\infty} \frac{\sigma^i}{i!}\,\mathcal{K}_i(y) \;\equiv\; \sum_{i=0}^{\infty} \frac{\sigma^i}{i!}\,\mathcal{H}_0^{(i)}(y),$$

through a generating function

$$\mathcal{W}(x;\sigma) \;=\; \sum_{i=0}^{\infty} \frac{\sigma^i}{i!}\mathcal{W}_{i+1}(x),$$

according to the recursion formula

$$\mathcal{H}_i^{(j)} \;=\; \mathcal{H}_{i+1}^{(j-1)} + \sum_{k=0}^{i} \binom{i}{k} \{\, \mathcal{H}_{i-k}^{(j-1)} \,,\, \mathcal{W}_{k+1} \,\}, \tag{72}$$

with $i \geq 0$, $j \geq 1$ and $\mathcal{H}_i^{(0)} = \mathcal{H}_i$ and $\{\,\cdot,\cdot\,\}$ denotes the Poisson bracket of two scalar fields, e.g. given $\mathcal{P}$ and $\mathcal{Q}$ the Poisson bracket is defined over an open domain of $\mathbb{R}^{2\,n}$ as the quantity

$$\{\,\mathcal{P}\,,\,\mathcal{Q}\,\} \;=\; \sum_{i=1}^{n} \left(\frac{\partial \mathcal{P}}{\partial x_i}\,\frac{\partial \mathcal{Q}}{\partial x_{i+n}} - \frac{\partial \mathcal{P}}{\partial x_{i+n}}\,\frac{\partial \mathcal{Q}}{\partial x_i} \right).$$

Notice that $x = (x_1, \ldots, x_{2\,n})$, where $(x_1, \ldots, x_n)$ stand for the coordinates and $(x_{n+1}, \ldots, x_{2\,n})$ refer to their conjugate momenta. Observe also that $\mathcal{W}(x;\sigma)$ is conserved under the transformation and thus, it can also be expressed as $\mathcal{W}(y;\sigma)$. The recursion process can be summarized in the so–called Lie triangle, see Figure 10.

Hence, Equation (72) yields now the partial differential identity

$$\mathcal{L}_{\mathcal{H}_0}(\mathcal{W}_i) + \mathcal{K}_i = \widetilde{\mathcal{H}}_i, \tag{73}$$

where $\widetilde{\mathcal{H}}_i$ collects all the terms known from the previous order and $\mathcal{L}_{\mathcal{H}_0}$ denotes the Lie operator (linear operator) associated to the Poisson bracket of two functions. More concretely, for two scalar fields P and Q defined over an open domain of $\mathbb{R}^{2\,n}$, we have that

$$\mathcal{L}_P(Q) = \{\, P \,,\, Q \,\}.$$

In identity (73), called the homology equation, $\mathcal{W}_i$ and $\mathcal{K}_i$ must be determined according to the specific requirements of the Lie transformation one performs.

The transformation $x = X(y;\sigma)$ relates the "old" variables x with the "new" ones y and is a near–identity change of variables. The direct change is given by

$$x \;\;=\;\; y + \sum_{i=1}^{\infty} \frac{\sigma^i}{i!}\, y_0^{(i)}. \tag{74}$$

The coordinates $y_0^{(i)}$, $i \geq 1$ are calculated recursively with the aid of

$$y_i^{(j)} \;=\; y_{i+1}^{(j-1)} + \sum_{k=0}^{i} \binom{i}{k}\, \{\, y_k^{(j-1)} \,,\, \mathcal{W}_{i+1-k} \,\}, \tag{75}$$

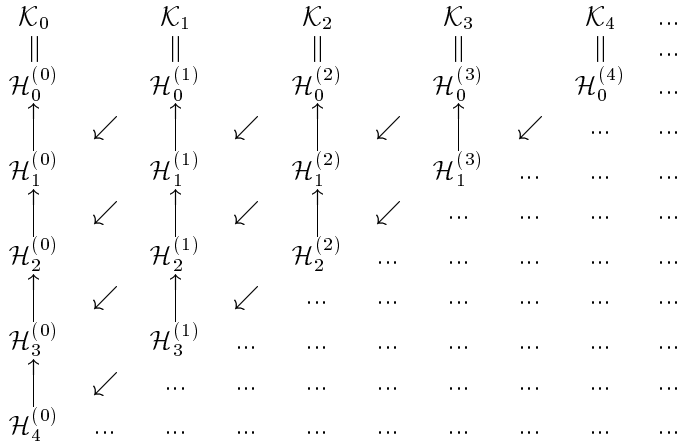

Figure 10: At each order $i \geq 1$ of the process, the diagonal $\mathcal{H}_j^{(k)}$ with $j+k=i$ is built starting with $\mathcal{H}_{i-1}^{(1)}$ and finishing with $\mathcal{H}_1^{(i-1)}$. Note that $\mathcal{H}_0^{(i)}$ cannot be determined unless $\mathcal{W}_i$ is previously known.

with $i \geq 0$, $j \geq 1$ and $y_i^{(0)} \equiv 0$ for $i \geq 1$ and $y_0^{(0)} \equiv y$. Consequently, Equation (74) gives the set of coordinates x in terms of y with the use of the generating function $\mathcal{W}$.

Similar formulae can be used to obtain the inverse transformation $y = Y(x;\sigma)$, which explicitly reads as

$$y \;=\; x + \sum_{i=1}^{\infty} \frac{\sigma^i}{i!}\, x_i^{(0)}. \tag{76}$$

Now $x_0^{(0)} \equiv x$ and for $i \geq 1$ coordinates $x_i^{(0)}$ are calculated recursively by means of

$$x_i^{(j)} \;=\; x_{i-1}^{(j+1)} + \sum_{k=0}^{i-1} \binom{i-1}{k} \{\, x_{i-k-1}^{(j)} \,,\, \mathcal{W}_{k+1} \,\}, \tag{77}$$

with $i \geq 1$, $j \geq 0$. This time $x_0^{(i)} \equiv 0$ for $i \geq 1$ and the Jacobians appearing in the operators of (77) are computed with respect to x and $\mathcal{W}_{k+1}$ is also written in x.

Note that Equation (74) can be used to transform any function expressed in the old variables x as a function of the new variables y. Similarly, Equation (76) is used to transform any function in y as a function of x. In this respect we can compute a formal integral of the original system by going back to the departure system. Specifically if the normal form calculations have been carried out to an order $M > 1$, then we determine $T^*(x;\sigma)$ as

$$T^*(x;\sigma) \;=\; T(x) + \sum_{i=1}^{M} \frac{\sigma^i}{i!}\, T(x)_i^{(0)}, \tag{78}$$

where $T(x)_i^{(0)}$ are calculated using

$$T(x)_i^{(j)} \;=\; T(x)_{i-1}^{(j+1)} + \sum_{k=0}^{i-1} \binom{i-1}{k} \{\, T(x)_{i-k-1}^{(j)} \,,\, \mathcal{W}_{k+1} \,\}, \tag{79}$$

with $i \geq 1$ and $j \geq 0$. Now $T(x)_0^{(0)} \equiv T(x)$ and for $i \geq 1$, $T(x)_0^{(i)} \equiv 0$. Then $T^*(x;\sigma)$ is an asymptotic symmetry of F, i.e. $\{\, F \,,\, T^* \,\} = \mathcal{O}(\sigma^{M+1})$. Details can be found in reference [43].

The above method is formal in the sense that the convergence of the various series is not discussed. Indeed, the series diverge for many applications. However, the lower orders of the transformed system can give interesting information and the process can be stopped at a certain order M. This means that these terms of the series are useful to construct both the transformed Hamiltonian and the generating function, since they are unaffected by the ultimately divergent character of the whole process.

3.3.2 Transformation to Normal Form Up to Order 6

We apply the Lie method to the complexified Hamiltonian $H' = \sum_{i=2}^{8} H_i$ where H_2 is given by (71) and each H_i, $i > 2$ is a homogeneous polynomial of degree i in the complex coordinates q and p obtained after expanding $1/\mathcal{R}$ in power series of q_i and p_i. Thus, our plan consists in carrying out the calculations up to polynomials of degree eight, e.g. up to sixth order in the normal form. In this way, we construct a change of coordinates from the old ones: $q = (q_1, q_2, q_3)$ and $p = (p_1, p_2, p_3)$ to the new ones: $q' = (q'_1, q'_2, q'_3)$ and $p' = (p'_1, p'_2, p'_3)$. We drop the primes to avoid tedious notation.

We start by identifying H_2 with $\mathcal{H}_0$ and each H_{i+2} with $\mathcal{H}_i/i!$, $i \leq 6$. Then, we must recall that terms belonging to $\widetilde{\mathcal{H}_i}$ are monomials in p and q of degree $i+2$ with real or complex coefficients c. So, a monomial of degree $i+2$: $m_i = c\, q_1^{j_1}\, q_2^{j_2}\, q_3^{j_3}\, p_1^{k_1}\, p_2^{k_2}\, p_3^{k_3}$ such that $\sum_{l=1}^{3}(j_l + k_l) = i+2$, belongs to the kernel of $\mathcal{L}_{H_2}$ (and therefore must be incorporated to the new Hamiltonian) if and only if $j_1 = k_1$, $j_2 = k_2$ and $j_3 = k_3$; otherwise its contribution to the new Hamiltonian is zero and the part corresponding to the generating function $\mathcal{W}_i$ becomes $m_i/(\mu\,(k_3 - j_3) + \imath\,(\omega_1\,(k_1 - j_1) + \omega_2\,(k_2 - j_2)))$. This is the key point in solving the homology equation (73) at each order i.

We rescale the coordinates, say $(q^*, p^*) \to \sigma\,(q, p)$, to introduce the small parameter σ and adopt then the formulae of Subsection 3.3.1. Afterwards we set $\sigma = 1$ and drop the stars to simplify our notation further. We call the normal form $K = \sum_{i=2}^{8} K_i$, and in diagonal complex coordinates (the transformed ones q' and p', that we have renamed q and p) reads as follows:

$$K(p,q) = \sum_{j,k,l}^{4} a(j,k,l)(p_1 q_1)^j (p_2 q_2)^k (p_3 q_3)^l, \tag{80}$$

with coefficients given by:

$a(1,0,0)$	$1.3292326209360146\,\imath$
$a(0,1,0)$	$1.9630114596221002\,\imath$
$a(0,0,1)$	1.2728995840709765
$a(2,0,0)$	$1.084118969828125 \times 10^{-1}$
$a(0,2,0)$	$6.432737304520157 \times 10^{-2}$
$a(0,0,2)$	$-2.412298516241746 \times 10^{-1}$
$a(1,1,0)$	$3.8502889530602764 \times 10^{-3}$
$a(1,0,1)$	$-5.709272495222898\,\imath \times 10^{-1}$
$a(0,1,1)$	$-4.029118438454696\,\imath \times 10^{-1}$
$a(3,0,0)$	$5.563568366758172\,\imath \times 10^{-3}$
$a(0,3,0)$	$-1.140865632382711\,\imath \times 10^{-3}$
$a(0,0,3)$	$-3.4607990223896906 \times 10^{-2}$
$a(2,1,0)$	$1.84708258092598\,\imath \times 10^{-2}$
$a(2,0,1)$	$-9.804116149675277 \times 10^{-2}$
$a(1,2,0)$	$-5.26869060648934\,\imath \times 10^{-2}$
$a(0,2,1)$	$-2.3139914837113457 \times 10^{-1}$
$a(1,0,2)$	$4.004377334411079\,\imath \times 10^{-2}$
$a(0,1,2)$	$2.76105499066869\,\imath \times 10^{-1}$
$a(1,1,1)$	$-9.949641599540471 \times 10^{-2}$
$a(4,0,0)$	$9.18992415784192 \times 10^{-3}$
$a(0,4,0)$	$3.921799630947499 \times 10^{-3}$
$a(0,0,4)$	$4.005710239128329 \times 10^{-2}$
$a(3,1,0)$	$1.2123807670174411 \times 10^{-2}$
$a(2,2,0)$	$1.1847669375067585 \times 10^{-2}$
$a(1,3,0)$	$2.5741638128707816 \times 10^{-2}$
$a(3,0,1)$	$-1.0660011034295587\,\imath \times 10^{-1}$
$a(2,0,2)$	$-3.307549676029244 \times 10^{-1}$
$a(1,0,3)$	$2.2562472925332147\,\imath \times 10^{-1}$
$a(0,3,1)$	$-6.01563793667196\,\imath \times 10^{-2}$
$a(0,2,2)$	$-1.7149257534732887 \times 10^{-1}$
$a(0,1,3)$	$3.281124863222212\,\imath \times 10^{-1}$
$a(2,1,1)$	$-2.4216727696341944\,\imath \times 10^{-1}$
$a(1,2,1)$	$2.2830888537513132\,\imath \times 10^{-2}$
$a(1,1,2)$	$-4.781394388287208 \times 10^{-1}$

(81)

Each H_i for $2 \leq i \leq 8$ in the last normal form Hamiltonian is a homogeneous polynomial of degree i. The generating function is also a polynomial in q and p of degree eight but it is too long to publish. Specifically, $\mathcal{W} = \sum_{i=1}^{6} \mathcal{W}_i/i!$ is written as $W = \sum_{i=3}^{8} W_i$ where each W_i is a homogeneous polynomial in (q,p) of degree i. Then, W_3 consists of 32 monomials, W_4 consists of 64 monomials, W_5 consists of 136 monomials, W_6 consists of 216 monomials, W_7 consists of 416 monomials and, finally, W_8 consists of 656 monomials.

Once W has been determined, we can calculate the new coordinates (or any function of them) as functions of the old ones and vice versa. This will be used in Section 3.4.

3.3.3 Three Formal Integrals

By the calculation of the normal form K the products $q_1\,p_1,\ q_2\,p_2,\ q_3\,p_3$ become integrals of the normalized Hamiltonian (the primes in the final step of the normalization are dropped here). Thus, after truncation at order 6 (e.g. truncation including eight–degree polynomials), we have transformed a three–degree–of–freedom system into a zero–degree–of–freedom one. These three integrals of K correspond to three asymptotic integrals of the Hamiltonian prior to normalization. Thus, the integrals of the original Hamiltonian are obtained with the aid of formula (78).

3.3.4 Exact Solutions for the Trajectories near the Transition State

We write the integrals in terms of the real normal form coordinates following (70) as follows:

$$\begin{aligned} J_1 &= \tilde{x}_1\tilde{P}_1 = q_3p_3, \\ J_2 &= \frac{1}{2}\left(\tilde{P}_2^2+\tilde{x}_2^2\right) = \imath q_2p_2, \\ J_3 &= \frac{1}{2}\left(\tilde{P}_3^2+\tilde{x}_3^2\right) = \imath q_1p_1. \end{aligned} \tag{82}$$

The truncated normal form Hamiltonian can be expressed entirely in terms of these integrals:

$$K = K(J_1, J_2, J_3). \tag{83}$$

Using (82) and the chain rule, Hamilton's equations can be written as follows:

$$\begin{aligned} \dot{\tilde{x}}_1 &= \frac{\partial K}{\partial \tilde{P}_1} = \frac{\partial K}{\partial J_1}\frac{\partial J_1}{\partial \tilde{P}_1} = \frac{\partial K}{\partial J_1}\tilde{x}_1, \\ \dot{\tilde{P}}_1 &= -\frac{\partial K}{\partial \tilde{x}_1} = -\frac{\partial K}{\partial J_1}\frac{\partial J_1}{\partial \tilde{x}_1} = -\frac{\partial K}{\partial J_1}\tilde{P}_1, \\ \dot{\tilde{x}}_2 &= \frac{\partial K}{\partial \tilde{P}_2} = \frac{\partial K}{\partial J_2}\frac{\partial J_2}{\partial \tilde{P}_2} = \frac{\partial K}{\partial J_2}\tilde{P}_2, \\ \dot{\tilde{P}}_2 &= -\frac{\partial K}{\partial \tilde{x}_2} = -\frac{\partial K}{\partial J_2}\frac{\partial J_2}{\partial \tilde{x}_2} = -\frac{\partial K}{\partial J_2}\tilde{x}_2, \\ \dot{\tilde{x}}_3 &= \frac{\partial K}{\partial \tilde{P}_3} = \frac{\partial K}{\partial J_3}\frac{\partial J_3}{\partial \tilde{P}_3} = \frac{\partial K}{\partial J_3}\tilde{P}_3, \\ \dot{\tilde{P}}_3 &= -\frac{\partial K}{\partial \tilde{x}_3} = -\frac{\partial K}{\partial J_3}\frac{\partial J_3}{\partial \tilde{x}_3} = -\frac{\partial K}{\partial J_3}\tilde{x}_3. \end{aligned} \tag{84}$$

It is important to note that $\frac{\partial K}{\partial J_i}$, $i = 1, 2, 3$, are constants on trajectories. Hence, once the initial condition of a trajectory is chosen, evolution of the trajectory is given by a linear system whose coefficients are constant, but depend on the trajectory.

This simple form of Hamilton's equations in the normal form coordinates near the transition state enables us to construct trajectories having any possible behavior near the transition state. These trajectories can then be visualized in the original coordinates using the transformation constructed in Section 3.4.

3.3.5 A Visualization Strategy in the Space of Integrals

Now we describe a visualization strategy *in the space of integrals*, which is a three-dimensional space with coordinates $J_1 - J_2 - J_3$. Since these integrals are constant on trajectories, a trajectory in this space corresponds to a point.

Energy Surface:

This is given by:

$$K(J_1, J_2, J_3) = h = \text{constant}. \tag{85}$$

This will typically be a two dimensional surface in the $J_1 - J_2 - J_3$ space, for each fixed h.

The NHIM and its Stable and Unstable Manifolds:

In the normal form coordinates the NHIM is given by $\tilde{x}_1 = \tilde{P}_1 = 0$, the stable manifold of the NHIM is given by $\tilde{x}_1 = 0$ and the unstable manifold of the NHIM is given by $\tilde{P}_1 = 0$. In the $J_1 - J_2 - J_3$ space these are all given by $J_1 = 0$. In other words, the NHIM and its stable and unstable manifolds are all identified with:

$$K(0, J_2, J_3) = h = \text{constant},$$

which is typically a curve in $J_1 - J_2 - J_3$ space.

The Transition State:

In the normal form coordinates this is given by $\tilde{x}_1 = \tilde{P}_1$; hence $J_1 \geq 0$. Therefore the transition state is given by:

$$K(J_1 \geq 0, J_2, J_3) = h = \text{constant}.$$

In this representation the transition state is a portion of the energy surface.

3.4 Transformation Back to the Original Coordinates

In order to construct the change of coordinates back to the original coordinates (i.e., $(\hat{x}_1, \hat{x}_2, \hat{x}_3, \hat{P}_1, \hat{P}_2, \hat{P}_3)$ of Eq. (53)) we make use of the generating function W. Indeed we simply have to evaluate Poisson brackets but without solving any partial differential equations. Therefore the computational effort is much smaller than the one corresponding to the calculation of the normal form Hamiltonian and the generating function.

With the inverse of the linear change given in (70) the complex formal integrals are transformed into real expressions as functions of $(\tilde{x}_1, \tilde{x}_2, \tilde{x}_3, \tilde{P}_1, \tilde{P}_2, \tilde{P}_3)$. As a final step we need to perform a new linear change of variables, inverting the matrix C and expressing consequently the three integrals in terms of $(\hat{x}_1, \hat{x}_2, \hat{x}_3, \hat{P}_1, \hat{P}_2, \hat{P}_3)$. We do not display the formulae of these integrals as they are quite long.

Next we build the direct change of coordinates $x = X(y; \sigma)$ given through formula (74). Notice that in this particular case x represents (q, p) and y stands for (q', p') (since we are explicitly discussing the transformation from the final step of the normalization back to the original coordinates we have returned the primes to the notation). Alternatively we can compute the change in real coordinates. For achieving this we first write W in real variables $(\tilde{x}', \tilde{P}') = (\tilde{x}'_1, \tilde{x}'_2, \tilde{x}'_3, \tilde{P}'_1, \tilde{P}'_2, \tilde{P}'_3)$ using the inverse of (70). Thence we calculate $(\tilde{x}, \tilde{P}) = (\tilde{x}_1, \tilde{x}_2, \tilde{x}_3, \tilde{P}_1, \tilde{P}_2, \tilde{P}_3)$ by means of (74). Note that on this occasion x in the formula $x = X(y; \sigma)$ means $(\tilde{x}, \tilde{P})$ whereas y represents $(\tilde{x}', \tilde{P}')$. With this second route $\tilde{x}_1$ is expressed as a function of 913 monomials in $(\tilde{x}', \tilde{P}')$, whereas $\tilde{x}_2$ consists

of 777 monomials and $\tilde{x}_3$ consists of 679 monomials. The momentum $\tilde{P}_1$ appears as a function of 913 terms in $(\tilde{x}', \tilde{P}')$, $\tilde{P}_2$ consists of 796 monomials and finally the formula for $\tilde{P}_3$ consists of 679 monomials in $(\tilde{x}', \tilde{P}')$.

3.5 Trajectories near the NHIM for the Hydrogen Atom in Crossed Electric and Magnetic Fields

We now show trajectories near the NHIM. In the normal form coordinates $J_1 = 0$ on the NHIM and its stable and unstable manifolds. Using (84) we can compute trajectories on the NHIM and on any branch of the stable and unstable manifold that we desire. Then these trajectories can be transformed back into the original coordinates. This is shown in Fig. 11 and Fig. 12. In each figure we take $J_3 = 1/2(\tilde{P}_3^2 + \tilde{x}_3^2) = 0.001$ and $J_2 = 1/2(\tilde{P}_2^2 + \tilde{x}_2^2) = 0.000953096$. In all of the figures the yellow trajectory is on the NHIM: $\tilde{P}_1 = \tilde{x}_1 = 0$.

The light green is the trajectory on the forward unstable manifold of the NHIM with $\tilde{P}_1 = 0$, $\tilde{x}_1 = 0.00001 \exp(1.2728t)$. The blue trajectory is on the backward unstable manifold of the NHIM with $\tilde{P}_1 = 0$, $\tilde{x}_1 = -0.00001 \exp(1.2728t)$.

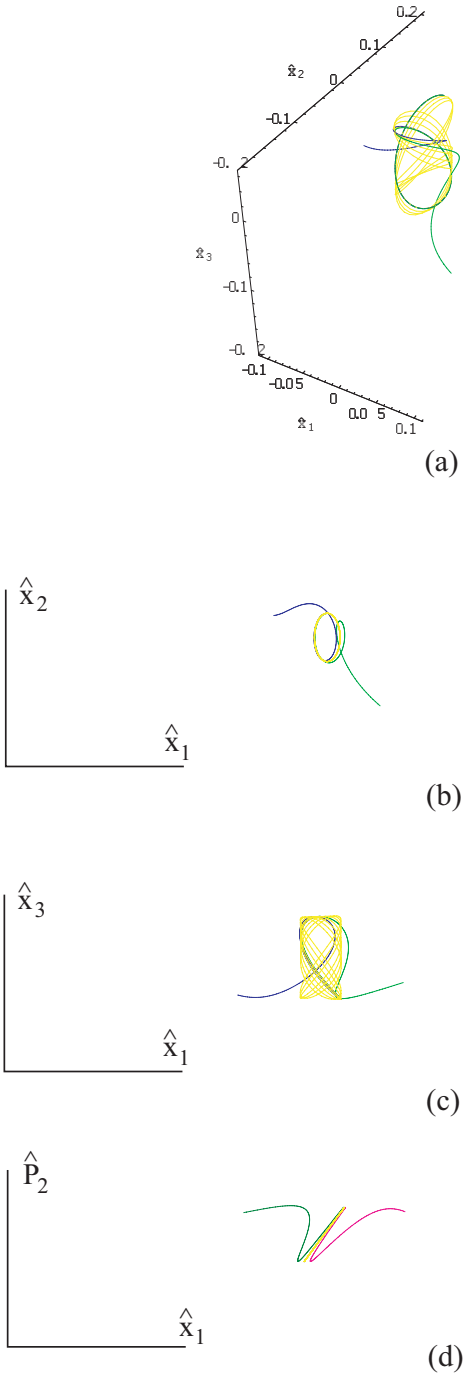

Figure 11: Different projections for trajectories in the NHIM and in the unstable manifold of the NHIM.

The dark green trajectory is on the forward stable manifold of the NHIM with $\tilde{P}_1 = 2\exp(-1.2728t)$, $\tilde{x}_1 = 0$. The pink trajectory is on the backward stable manifold of the NHIM with $\tilde{P}_1' = -2\exp(-1.2728t)$, $\tilde{x}_1 = 0$.

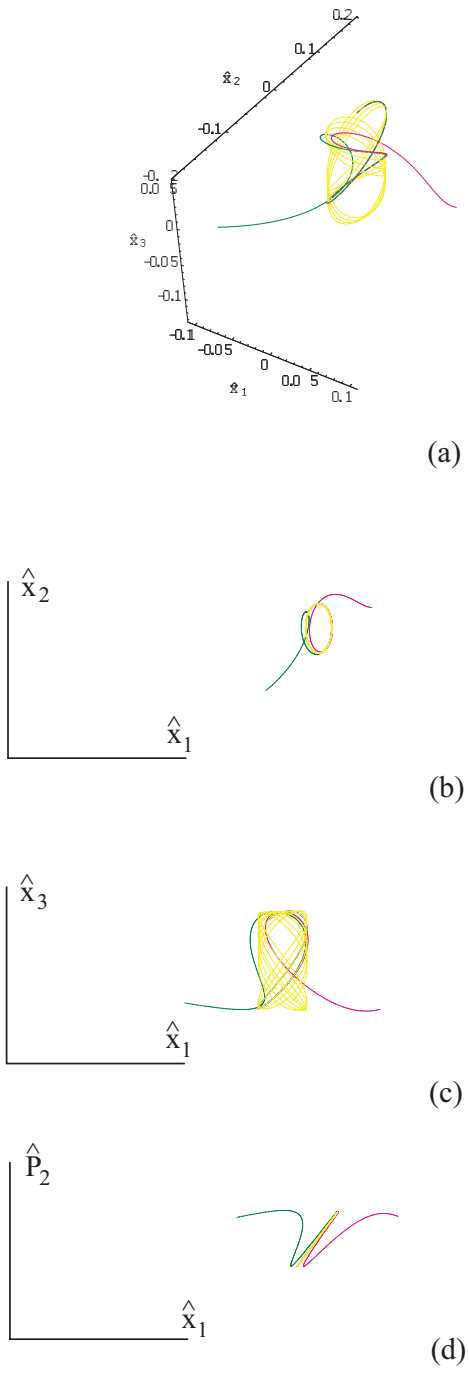

Figure 12: Different projections for trajectories in the NHIM and in the stable manifold of the NHIM.

The significance of our ability to compute these trajectories should not be undervalued. The normal form coordinates give us the ability to compute trajectories that would be almost impossible to compute in the original coordinates. For example, we can compute trajectories that start on the

three dimensional normally hyperbolic invariant manifold in the five dimensional energy surface. We can compute trajectories in either the forward or backward stable and unstable manifolds. These trajectories are simply chosen and computed for the normal form vector field (84). The normal form transformation then allows us to visualize them in the original coordinates. In other words, we have complete control and knowledge of the exact dynamical trajectories near the transition state in a 3 dof system. This is the first time this has been demonstrated for a 3 dof chemical or atomic system.

4 Summary and Outlook

The problem solved in this paper is the construction of hypersurfaces of no return in the *phase space* of strongly coupled, multidimensional systems. Our solution leads naturally to the multidimensional generalization of a saddle "point" and its associated separatrices. Indeed, this paper makes explicit the long-sought classical structures that act as transition states in phase space beyond 2dof. We show that the rigorous way to describe the notion of a "barrier" in phase space is through invariant manifolds.

Until very recently, neither the theoretical understanding nor the computing power was adequate to explore phase-space transport beyond the well-known two degrees-of-freedom ('2dof') limit [7]. However, using the recent advances in dynamical systems theory [60], especially concerning Normally Hyperbolic Invariant Manifolds (NHIM)[61], the classical theory of chemical reactions has been anchored rigorously in nonlinear dynamics by this paper.

References

[1] V. I. Arnol'd, V. V. Kozlov, and A. I. Neishtadt, *Mathematical Aspects of Classical and Celestial Mechanics* (Springer-Verlag, New York, 1988).

[2] P. Bellomo, D. Farrelly, and T. Uzer, J. Phys. Chem. A **101**, 8902 (1997).

[3] A. Bohr and B. R. Mottelson, *Nuclear Structure, Vol. II* (Benjamin Reading, MA 1975).

[4] P. A. Braun and E. A. Solov'ev, Sov. Phys JETP **59**, 38 (1984).

[5] J. P. Connerade, *Highly Excited Atoms* (Cambridge University Press, Cambridge, UK, 1998).

[6] M. J. Davis and E. J. Heller, J. Chem. Phys. **75**, 2461 (1980).

[7] M. J. Davis, J. Chem. Phys. **83**, 1016 (1985); M. J. Davis, J. Chem. Phys. **86**, 3978 (1987); M. J. Davis and S. K. Gray, J. Chem. Phys. **84**, 5389 (1986); S. K. Gray, S. A. Rice, and M. J. Davis, J. Phys. Chem. **90**, 3470 (1986); M. J. Davis, J. Phys. Chem. **92**, 3124 (1988).

[8] D. Delande and J.-C. Gay, in *The Hydrogen Atom*, edited by G. Bassani, M. Inguscio, and T. Haensch (Springer-Verlag. Berlin, 1989), pp. 323-334.

[9] A. Deprit, Celestial Mechanics **1**, 12 (1969).

[10] M. M. Dignam and J. E. Sipe, Phys. Rev. B **45**, 6819 (1992).

[11] B. Eckhardt, Phys. Rep. **163**, 205 (1988).

[12] B. Eckhardt, J. Phys. A: Math. Gen. **28**, 3469 (1995).

[13] H. Eyring, J. Chem. Phys. **3**, 107 (1935).

[14] H. Eyring and M. Polanyi, Z. Physik. Chem. B **12**, 279 (1931).

[15] D. Farrelly, Phys. Lett. A **191**, 265 (1994).

[16] W. Forst, *Theory of Unimolecular Reactions* (Academic, New York, 1973); P. J. Robinson and K. A. Holbrook, *Unimolecular Reactions* (Wiley, New York, 1992).

[17] R. R. Freeman and D. Kleppner, Phys. Rev. A **14**, 1614 (1976).

[18] H. Friedrich and D. Wintgen, Phys. Rep. **183**, 37 (1989).

[19] T. F. Gallagher, *Rydberg Atoms* (Cambridge University Press, Cambridge, UK, 1994).

[20] M. Gutzwiller, *Chaos in Classical and Quantum Mechanics* (Springer-Verlag, New York, 1990).

[21] H. Hasegawa, M. Robnik, And G. Wunner, Prog. Theor. Phys. Suppl. **98**, 198 (1989).

[22] R. Hernández and W. H. Miller, Chem. Phys. Lett. **214**, 129 (1993).

[23] G. Herzberg, Annu. Rev. Phys. Chem. **38**, 27 (1987).

[24] R. J. Hinde and R. S. Berry, J. Chem. Phys **99**, 2942 (1993); T. Komatsuzaki and R. S. Berry, *ibid* **110**, 9160 (1999).

[25] J. O. Hirschfelder and E. Wigner, J. Chem. Phys. **7**, 616 (1939).

[26] J. Horiuti, Bull. Chem. Soc. Japan **13**, 210 (1937).

[27] C. Jaffé, D. Farrelly, and T. Uzer, Phys. Rev. Lett. **84**, 610 (2000); Phys. Rev. A **60**, 3833 (1999).

[28] B. R. Johnson, J. D. Hirschfelder, and K. H. Yang, Rev. Mod. Phys. **55**, 109 (1983).

[29] J. C. Keck, Adv. Chem. Phys. **13**, 85 (1967).

[30] For reviews see, e.g., J. C. Keck, Adv. Chem. Phys. **13**, 85 (1967); D. G. Truhlar, J. Phys. Chem. **100**, 12271 (1996).

[31] S. Keshavamurthy and W. H. Miller, Chem. Phys. Lett. **205**, 96 (1993).

[32] P. M. Koch and K. A. H. van Leeuwen, Phys. Rep. **255**, 289 (1995).

[33] G. W. Koeppl, J. Am. Chem. Soc. **96**, 6539 (1974).

[34] R. S. MacKay, Phys. Lett. A **145**, 425 (1990); Nonlinearity **4**, 155 (1991).

[35] J. Main and G. Wunner, Phys. Rev. Lett. **69**, 586 (1992).

[36] J. Main and G. Wunner, J. Phys. B **27**, 2835 (1994).

[37] A. Marcelin, Ann. Chim. Phys **3**, 158 (1915).

[38] G. Mathys, Fundamentals of Cosmic Physics **13**, 143 (1989).

[39] F. Mignard, Icarus **49**, 347 (1982).

[40] W. H. Miller, Faraday Discuss. Chem. Soc. Lond. **62**, 40 (1977).

[41] W. H. Miller, Faraday Discuss. Chem. Soc. Lond. **110**, 1 (1998).

[42] A. M. Ozorio de Almeida, N. de León, M. A. Mehta, and C. C. Marston, Physica D **46**, 265 (1990).

[43] J. Palacián and P. Yanguas, Nonlinearity **13**(4), 1021 (2000).

[44] P. Pechukas, in *Dynamics of Molecular Collisions,* Part B, W. H. Miller, Ed. (Plenum Press, N. Y., 1976), chap. 6.

[45] P. Pechukas and F. J. McLafferty, J. Chem. Phys **58**, 1622 (1973); E. Pollak and P. Pechukas, *ibid* **69**, 1218 (1978); P. Pechukas and E. Pollak, *ibid* **71**, 2062 (1979).

[46] E. Pollak, in *Theory of Chemical Reactions*, M. Baer, Ed. (CRC Press, Boca Raton, FL, 1985), chap. 2.

[47] G. Raithel, M. Fauth, and H. Walther, Phys. Rev. A **44**, 1898 (1991).

[48] G. Raithel, M. Fauth, and H. Walther, Phys. Rev. A **47**, 419 (1993).

[49] G. Raithel and H. Walther, Phys. Rev. A **49**, 1646 (1994).

[50] P. Schmelcher, Phys. Rev. B **48**, 14642 (1993).

[51] E. A. Solov'ev, Sov. Phys. JETP **58**, 63 (1983).

[52] A. Tiyapan and C. Jaffé, J. Chem. Phys. 99, 2765 (1993); J. Chem. Phys. 101, 10393 (1994); J. Chem. Phys. 103, 5499 (1995).

[53] M. Toller, G. Jacucci, G. DeLorenzi, and C. P. Flynn, Phys. Rev. B **32**, 2082 (1985).

[54] T. Uzer, Phys. Script. **T90**, 176 (2001).

[55] T. Uzer and D. Farrelly, Phys. Rev. A **52**, R2501 (1995).

[56] T. Uzer, E. Lee, and D. Farrelly, Phys. Rev. A **58**, 4761 (1998).

[57] J. von Milczewski, G. H. F. Diercksen, and T. Uzer, Phys. Rev. Lett. **73**, 2428 (1994).

[58] J. von Milczewski and T. Uzer, Phys. Rev. E **55**, 6540 (1997).

[59] G. Wiebusch *et. al.*, Phys. Rev. Lett. **62**, 2821 (1989).

[60] S. Wiggins, *Chaotic Transport in Dynamical Systems* (Springer-Verlag, New York, 1992).

[61] S. Wiggins, *Normally Hyperbolic Invariant Manifolds in Dynamical Systems* (Springer-Verlag, New York, 1994).

[62] S. Wiggins, L. Wiesenfeld, C. Jaffé, and T. Uzer, Phys. Rev. Lett. **86**(24), 5478 (2001).

[63] E. P. Wigner, J. Chem. Phys. **5**, 720 (1937).

[64] E. P. Wigner, Trans. Faraday Soc. **34**, 29 (1938).